GINNA NUCLEAR POWER PLANT

ROCHESTER GAS AND ELECTRIC CORPORATION

316(a) DEMONSTRATION SUPPLEMENT

NPDES PERMIT NO.070 0X2 2 000079
(NY 0000493)

MARCH 1977

TABLE OF CONTENTS

GINNA 316(a) DEMONSTRATION SUPPLEMENT

INTRODUCTION

This document (Supplement) supplements the data and information submitted to the U.S. Environmental Protection Agency (EPA), Region II, on July 30, 1974, in support of a Section 316(a) application for the Ginna Nuclear Power Plant (Application No. 070 0X2 2 000079; NY 0000493) for alternate effluent limitations pursuant to Section 316(a) of the Federal Water Pollution Control Act Amendments of 1972 (FWPCA).

The July 30, 1974 Ginna 316(a) application containing a Demonstration Type I (absence of prior harm) was prepared and submitted to EPA, Region II in a 90-day period required by the draft Section 402 permit dated May 22, 1974 for the Ginna Nuclear Power Plant issued by EPA in accordance with proposed effluent limitations and standards of performance for steam electric generating facilities (Proposed 40 CFR Part 423, 39 Fed. Reg. 8293, March 4, 1974). This submission was further supplemented on August 23, 1974 by a Demonstration Type II (protection of representative important species). Those proposed regulations required closed cycle cooling for existing power plants of the Ginna Power Plant size category or, alternatively, an exemption authorizing once-through cooling system related discharge limitations under criteria established under Section 316(a) of the FWPCA. That Ginna 316(a)

application was filed but not formally processed by EPA since in November of 1974 final regulations for the steam electric generating plant source category eliminated the requirement for closed cycle cooling for existing facilities below 500 MW, which excluded the Ginna Plant.

A final permit was issued by EPA for the Ginna Nuclear Power Plant on February 24, 1975, and portions of this permit were contested in an adjudicatory hearing request submitted pursuant to the requirements of 40 CFR Part 125. The issues subject to adjudicatory hearing proceedings, including numerous thermal issues, are specified in a letter from Meyer Scolnick of EPA dated May 15, 1975, to Robert R. Koprowski of RG&E. With regard to the thermal issues, the final permit required closed cycle cooling in the absence of a demonstration that the facility was not required to meet the 3°F discharge limitation on discharges to lakes contained in New York State thermal water quality standards and criteria. (6 NYCRR Part 704.) The contention related to the thermal provisions involved, first, the authority of EPA to disapprove (or "exempt from consideration") certain portions of 6 NYCRR Part 704 which would have clearly exempted the Ginna Plant from the 3°F limitation and, second, the authority of EPA, Region II (as opposed to the State of New York) to establish a mixing zone for the 3°F isotherm.

EPA, RG&E and the New York State Department of Environmental Conservation (DEC) have participated in efforts to reach a resolution of the thermal and other permit issues prior to the opening of adjudicatory hearings. Several conferences have taken place among EPA, RG&E and DEC representatives and numerous telephone conferences and correspondence have been exchanged between the parties.

An agreement in principle has been reached with EPA with regard to the settlement of issues raised in the adjudicatory hearing request, although the settlement has not been finalized in formal stipulation documents. The settlement agreement includes resolution of the thermal issues described above. Without conceding the validity of their respective legal positions, RG&E, EPA, Region II and the DEC determined that adjudication of legal questions on the State's thermal standard and criteria and the role of EPA in the implementation of them would not be necessary if it could be shown with reasonably available information that the Ginna Plant is entitled to operate with the once-through cooling system now utilized at that facility. Assuming EPA and DEC agreement on the feasibility of the existing system, the avoidance of potentially lengthy adjudication and the expectation of a State desire to review reasonably available information on the effect of the Ginna Plant in any event, a settlement seemed particularly appropriate.

Among the provisions of the settlement reached on the thermal contentions described above was an agreement by EPA to issue a "no-action"letter , that is a letter by which EPA agrees to exercise its prosecutorial discretion to refrain from enforcement action against RG&E for failure to achieve any of the thermal limitations in the Section 402 permit while further resolution of the thermal issues is pending before the agency. As a condition of EPA's agreement not to initiate enforcement action in this regard, RG&E agreed to submit this Supplement on or before March 31, 1977. RG&E has chosen not to withhold submission of this Supplement even though the promised "no-action" letter is not in hand. However, this Supplement is submitted contingent on receipt by RG&E of the above mentioned "no-action" letter containing provisions which do not differ significantly from those discussed orally between the parties during settlement conferences. In the event either that the "no-action" letter is not issued or that, when issued, its contents do not comport with prior understandings, this Supplement is subject to withdrawal by RG&E. Further, RG&E reserves the right to contest by 40 CFR Part 125 procedures the Section 316(a) determinations ultimately rendered on the Applicant's Section 316(a) submittals, including the right to raise any of the thermal contentions

now pending in the adjudicatory hearing proceedings for the Ginna Nuclear Power Station. It should be noted that this right is specifically recognized in stipulations to be signed in settlement of the Section 402 permit issues.

In the course of conferences convened to resolve the thermal issues raised in the adjudicatory hearing request, EPA requested additional information from RG&E with regard to its 316(a) showing, since, subsequent to submission of RG&E's 316(a) report on July 30, 1974, as supplemented on August 23, 1974, EPA has published additional information on the subject of 316(a) demonstration evidence.

RG&E agreed to submit the requested additional information in this Supplement in accordance with guidelines set forth in a letter dated November 9, 1976 from Harvey Lunenfeld of EPA Region II to Roger W. Kober of RG&E. In addition to the specifications provided in this letter, this Supplement has been prepared on the basis of agreement between RG&E and the EPA Staff with regard to the definition of the scope of information to be provided in this Supplement as well as the appropriate format for its presentation. In some instances, RG&E has incorporated by reference discussions from its Section 316(a) and Section 316(b) demonstration for the Sterling Nuclear Power Plant. This document is entitled "The Sterling Power Project -

Nuclear Unit No. 1, Volume 4 - Water Permits" and copies thereof have been provided to EPA, Region II. This procedure is used with the expressed approval of EPA.

Finally, it is recognized that there may be some inconsistency between this Supplement and the Section 316(a) document submitted on July 30, 1974. Wherever this Supplement is inconsistent with the previous document, the statements in this Supplement shall supersede those in the 1974 document. This Supplement references two additional years (1974 and 1975) of ecological studies at the Ginna site and summarizes effects of Ginna operations upon the Representative Important Species over the period 1969 to 1975. Data used for verification of thermal plume modelling includes 1976 lake triaxial studies.

TABLE OF CONTENTS

CHAPTER 1: THERMAL PLUME CHARACTERISTICS

TABLE OF CONTENTS

CHAPTER 1 (Continued)

LIST OF TABLES

LIST OF FIGURES

LIST OF FIGURES (continued)

LIST OF FIGURES (continued)

LIST OF FIGURES (continued)

LIST OF FIGURES (continued)

LIST OF FIGURES (continued)

SUMMARY AND CONCLUSIONS

Ginna Nuclear Power Plant
316(a) Demonstration Supplement

The following statements are summaries and conclusions of the data and material contained in this document. Section numbers, which present complete discussions of the bases or reasons for each statement, are included in parenthesis.

1. The water quality related discharges from the Ginna Plant are governed by a final National Pollutant Discharge Elimination System (NPDES) permit issued for this facility in February, 1975. The Ginna Plant discharges are in compliance with all chemical limitations specified in that permit. The purpose of this report is to provide supplemental information necessary for the determination of the thermal limitations for the existing discharge. (Introduction)

2. The Ginna Nuclear Power Plant is licensed to permit operations at power levels up to 1520 MWt. A pressurized-water reactor (PWR) is used to produce thermal energy. A steam turbine-generator uses this heat to provide 490 MWe (net) of electrical power output. (1.1)

3. Heat-removal facilities for normal operation consists of a conventional once-through system with cooling water being withdrawn from and returned to Lake Ontario. The total circulating water flow of 400,000 GPM is withdrawn through a submerged octagonal intake structure that lies some 3100 ft offshore in about 35 ft of water and is returned to the lake via a canal as a shoreline surface discharge. Retention time of condenser cooling water in the plant system is about eight minutes. (1.2)

4. The waste heat released to Lake Ontario by the plant is about 4.0×10^9 BTU/HR at 490 MWe of rated output. The 400,000 GPM flow is normally maintained at all power levels. A temperature increase of 20F° has been assumed across the condenser cooling and service water systems for calculations of waste heat rejection. (1.3.1)

5. A dimensionless empirical model of a heated surface discharge into shallow water was derived. Five years of thermal survey data at the Ginna site were used to determine the model constants. Both surface and six foot depth thermal distributions were simulated. (1.4.1.1)

6. The model was compared with both the five years of thermal survey data used to determine the model constants plus eight independent surveys not used in the model development. Good agreement was found. (1.4.1.2)

7. Bottom temperatures (1.4.2.2) and velocities (1.4.3.1.2), based on field measurements, were also simulated. 3°F bottom contact occurs within approximately 1000 feet of shore (1.4.2.2). Lake bottom scour areas are less than 5 acres (1.4.3.1.2).

8. Seasonal expected and extreme ambient conditions were found (1.4.2.1). The thermal effects of the Ginna discharge during each seasonal condition were simulated. The largest thermal effects, exclusive of winter conditions, were generally found in the spring (1.4.2.5). The expected 3°F spring isotherm has areas on the lake surface, 6 foot depth, and bottom of 86, 32, and 5.6 acres, respectively. (1.4.3.5.1.2)

9. Winter effects, although not explicitly modelled were estimated based on mechanistic considerations (1.4.2.4). The winter plume was found to be of the same general size as the other seasonal plumes (1.4.2.5.1.1, 1.4.2.5.2.1).

10. Segmental impact zones to the 3°F isotherm are utilized as a basis for the areal assessment of any thermal impacts upon the aquatic ecosystem. Zones of impact are classified as a DISCHARGE ZONE and and MIXING ZONE. The DISCHARGE ZONE is evaluated quantitatively due to the high frequency of plume occurrence. The MIXING ZONE is addressed on a qualitative basis due to its low probability of occurrence. The area of the DISCHARGE ZONE at the surface, 6 foot depth, and bottom is 176, 65 and 11 acres, respectively. The zones of impact defined herein conservatively exceed the areal dimensions of the expected and extreme thermal plumes of the Ginna discharge. (1.5)

11. Representative Important Species (RIS) designated for the aquatic ecosystem at the Ginna site are Cladophora, Gammarus, Alewife, Smelt, Spottail Shiner, Smallmouth Bass, White Perch, Coho Salmon and Brown Trout. Rationale for selection of these species is provided in discussions contained in the Sterling 316(a) Demonstration and incorporated herein by reference (2.0).

12. The macroflora community at Ginna Station is composed entirely of Cladophora glomerata, the abundance of which decreases lakeward and is essentially absent by six meters of water depth. Cladophora demonstrates random yearly abundances, with the variance among years at each transect greater than the variance among transects for each year. A lasting effect of the discharge cannot be detected (3.1).

13. The macroinvertebrate community, represented by Gammarus, shows typically greater concentrations at the two and five meter depths, diminishing lakeward from the five meter depth. No significant differences in abundance have been found between the transects even though the distribution of Gammarus appears to be patchy. Annually, abundances of Gammarus are relatively stable. The discharge does not seem to have an adverse impact on this community (3.2).

14. The fish net studies conducted at the Ginna site from 1969 through 1975 have supplied information upon which the RIS fish have been chosen. These species, listed in order of decreasing Catch per Unit Effort (CUE), are: Alewife, White Perch, Spottail Shiner, Rainbow Smelt, Smallmouth Bass, Brown Trout and Coho Salmon. Each RIS fish population at the Ginna Site has been analyzed with respect to general distribution and abundance, relationship to the thermal plume based on perference temperatures and swimming abilities, attraction to or avoidance of the plume based on collected data, use of the site as a spawning or nursery area, and yearly fluctuations in abundance. A final section deals with all of the above areas on a total RIS-fish community basis. (3.3)

15. Seasonal preference temperatures and swimming capabilities for each RIS fish are discussed relative to acclimation temperature and other modifying factors. These data are variously utilized in other sections to both predict and verify actual responses of fish to the Ginna discharge, and to determine their potential for plume penetration and possible impact (3.3.3.2, 3.3.4.2, 3.3.5.2, 3.3.6.2, 3.3.7.2, 3.3.8.2.3.3.9.2).

16. RIS fish show varying degrees of attraction to and avoidance of the thermal plume during the course of the year based upon an Attraction Index. All species appear to behave generally in good agreement with their thermal preferenda and migratory instincts. This results in apparently minor effects upon the RIS fish community, in that these species fluctuate seasonally, showing that natural behavior patterns are dominant over influences of the thermal plume (3.3.10.2).

17. Fish egg and larvae studies have identified the following RIS-fish larvae at the Ginna site: alewife, smelt, white perch and shiners. Utilization of the site as a spawning or nursery area is assumed to be predominated by alewives, while other species may use it sporadically. Some species (coho salmon and brown trout) are not assumed to be able to naturally reproduce in Lake Ontario or its tributaries. Spawning intensity seems normal for each RIS in accordance with their species-specific habitat requirements. The area does not appear to be a preferred or unique spawning or nursery area for any RIS-fish. (3.3)

18. A quantitative assessment of theoretical thermal impact, expressed in terms of time and areas within the discharge zone from which organisms might be excluded, is provided for each RIS. Exclusion areas occur either at the surface, six-foot depth, or region of plume bottom-contact, depending upon the behavior and habitat of each species; they represent portions of the discharge zone where upper thermal tolerances are exceeded for various life activities such as parent survival, summer survival, growth (optimal and acceptable), reproduction, and development (4.1, 4.2).

Species - specific conclusions derived from this theoretical approach are as follows:

Macroflora (Cladophora) - Considering the extremely small areas of bottom contact (less than six acres) and time in summer when parent stock may be excluded, and considering the absence of potential thermal impact on all remaining life activities outside from the scour zone, it is reasonable to expect the Ginna plume to have a negligible adverse impact on Cladophora (4.2.1).

Macroinvertebrates (Gammarus) - Given the absence of potential thermal impact on survival of adult gammarids, the extremely small areas of plume bottom - contact and brief periods of impact on eggs, immatures, and reproduction, and lastly the predicted suboptimal growth within a small area during summer, it appears unlikely that the Ginna discharge could have a significant, much less a measureable, adverse thermal impact on Gammarus, hence the macroinvertebrate community (4.2.2).

Fish (Alewife)-- To summarize potential thermal effects of the Ginna discharge upon alewives, the applicant anticipates a small area of possible exclusion for mature fish in July, very small areas consistently or larger areas for brief time periods excluding juveniles in summer, suboptimal growth in various portions of the discharge zone mostly in summer (assuming alewives remain there for weeks or months), and finally negligible thermal impact on their development and reproduction activities. On this basis the applicant concludes no appreciable adverse thermal impact on the alewife population (4.2.3.1).

(Smelt) - Due to smelt's preference for cold water, and its normal distribution in deep, offshore waters in the summer, the potential for thermal impact on this species is expected to be minimal. Reproduction and development activities would not be thermally impacted apart from the maximum scour zone (4.2.3.2).

(Spottail Shiner) - The applicant anticipates no consequential thermal effects on either reproduction, development, or parent survival of spottail shiners within the Ginna discharge zone. The potential for direct impact on spottails, and suboptimal growth within various sized areas in summer, is minimized by their general avoidance of the nearshore area at this time (4.2.3.3).

(White Perch) - The applicant finds no potential thermal impact on reproduction, development, and parent survival within the Ginna discharge zone. There is a potential for some exclusion of white perch from small areas during the warmest part of summer, and a potential for suboptimal growth in areas of various dimensions during the summer months. Enhancement of food reserves in and about the discharge may compensate for thermally induced suboptimal growth, and serve to minimize the extent of potential impact (4.2.3.4).

(Smallmouth Bass) - To summarize the findings of a theoretical thermal impact assessment on various life activities of smallmouth bass, one could safely conclude that the Ginna discharge has a negligible impact on development, reproduction, and parent survival, and would exclude individuals from inhabiting very small areas (less than 3.5 percent of the discharge zone) during the summer. Growth could be suboptimal within reasonably small subsurface areas, however enhanced availability of food resources may compensate for such potential effects (4.2.3.5).

(Coho Salmon) - The applicant's evaluation of theoretical thermal impact on coho salmon of Lake Ontario, has demonstrated a low potential for impact on mature forms migrating through the region beneath the discharge zone in late summer and October, and a minimum potential impact on acceptable growth of individuals occupying the discharge zone in spring and fall (4.2.3.6).

(Brown Trout) - The results of a theoretical impact assessment on brown trout at Ginna suggest no impact on mature specimens occupying nearshore waters in the fall, though there is a possible exclusion from a small area of the discharge zone should some individuals migrate shoreward earlier (September). The potential for impact on growth (optimal and acceptable) should be greatly minimized in summer since brown trout occupy waters somewhat offshore within their preferred temperature range. No significant impact is predicted on growth in late spring. Successful reproduction and development of this stocked species is questionable in Lake Ontario; therefore the applicant anticipates no potential for thermal impact on these activities (4.2.3.7).

19. A species-specific evaluation of cold-shock effects, stemming from a reactor shutdown (rapid or scheduled), indicates a potential for low impact and a confinement of possible effects to specific colder months. Minimal concentrations of rainbow smelt, coho salmon, and brown trout might experience cold-shock during winter; spottail shiners and white perch could be stressed and/or cold-shocked only in February; alewives are prone to impact mainly in April; and smallmouth bass are never expected to experience cold-shock. In general, the extent of potential impact would be slight based on the few individuals inhabiting discharge waters during cold months, and is not expected to adversely affect protection and propagation of RIS fish at Ginna (4.2.3.1-7).

20. The plume entrains local lake water and transports it out into the lake. This offshore transport of lake water is replaced by an equal onshore movement of water. Such a countercurrent is usually found beneath the plume and has its origins offshore of the plume area. The flow rate of water entrained into the plume was calculated as a function of temperature and plume location. The maximum flow of entraining water exposed to 3°F temperatures or higher with expected spring conditions is approximately 2700 cfs (5.1.1).

21. Numbers of organisms which may be entrained into the plume have been estimated based upon: (1) the concentrations of fish eggs and larvae and the RIS-Gammarus found at the Ginna site, and (2) calculations of the volume of water entrained. These estimates are presented for the period of May through September which would be the period of highest concentrations for such organisms. Considerations and findings of this plume entrainment assessment include: (1) evidence of a limnetic countercurrent which flows shoreward beneath the thermal plume which may significantly reduce entrained organisms, (2) an insignificant thermal stress imposed upon Gammarus and a slight displacement of some of these organisms, (3) minor entrainment of fish eggs since most found near the Ginna site are dimersal, and (4) indications that larvae entrained into the plume would not reach detrimental temperatures. Overall, entrainment into the thermal plume has not be determined to result in adverse impact upon the RIS (5.1.2).

22. Fish tagging studies conducted from 1973 through 1976 support evidence that little, if any, interference to fish movements along shore may be attributed to the Ginna thermal discharge into Lake Ontario (5.2).

23. Gas bubble disease (GBD), a condition which may develop in fish subjected for a critical species-specific period of time to discharge waters supersaturated with a critical concentration of total gases and/or threshold ratio of dissolved oxygen to nitrogen, has neither been, nor is expected to be, a problem at the Ginna discharge. Support for this conclusion is derived from studies on L. Michigan where it was demonstrated that sensitive species such as brown trout, coho salmon, spottail shiners and others, captured from supersaturated discharge waters, did not exhibit symptoms of GBD. The author attributes these findings to short residence times of fish in critical areas of potential impact. This behavior, coupled with a paucity of fish observed occupying discharge waters at Ginna during critical periods (mainly winter months), greatly minimizes potential impact. Actual observed occurrences of GBD at the Ginna site have been rare (5.3).

This supplement demonstrates that the shoreline surface discharge of the Ginna Nuclear Power Plant assures the protection and propagation of a balanced indigenous aquatic community as exemplified by the Representative Important Species at the Ginna Site.

CHAPTER 1.0

THERMAL PLUME CHARACTERISTICS

1.1 PLANT DESCRIPTION

The Ginna Nuclear Power Plant is located on Lake Ontario in the northwest corner of Wayne County, N.Y. This location, on the south shore of Lake Ontario, is about 20 miles ENE of Rochester, N.Y. and 45 miles WSW of Oswego, N.Y. Figure 1.1-1 shows the counties and the larger cities and towns within 50 miles of the site. The nearest planned and existing nuclear facilities are located at the Sterling site (about 34 miles away) and Nine Mile Point Units (about 49 miles away), respectively.

Rochester Gas and Electric Corporation (RG&E) obtained its provisional license on September 19, 1969 to operate Ginna at 1300 megawatts thermal (MWt). The AEC Directorate of Licensing amended this provisional operating license to RG&E on March 1, 1972 to allow operation at power levels up to 1520 MWt. A pressurized-water reactor (PWR) is used to produce this thermal power level. A steam turbine-generator uses this heat to provide 490 MWe (net) of electrical power capacity.

The plant consists of a closed-cycle, pressurized, light-water-moderated nuclear steam-supply system, a turbine-condenser system, and auxiliary equipment. Figure 1.1-2 is a simplified flow diagram of the steam-electric system. After passing through the turbines, spent steam is condensed by once-through cooling with water from Lake Ontario. At full design power, the plant removes water from Lake Ontario at the rate of 400,000 GPM and heats it to a temperature 20F° above ambient lake temperature before returning it to the lake as a shoreline surface discharge.

1.2 HEAT DISSIPATION SYSTEM DESCRIPTION

Heat-removal facilities for normal operations consist of a conventional once-through system with cooling water being withdrawn from and returned to the same waterbody. The intake-discharge facilities are designed to provide the water requirements for the circulating water system and the house service water system. The total flow of circulating water through these systems under normal operating conditions is about 400,000 GPM (891.2 CFS). Figure 1.2-1 is a flow diagram of these once-through systems. Lake Ontario is the

source and recipient of the circulating water which is withdrawn through a submerged octagonal intake structure that lies some 3100 ft offshore in about 35 ft of water. Figure 1.2-2 is a perspective drawing of the intake structure, screenhouse and discharge canal. Intake water flows by gravity through a 10 ft diameter concrete-lined tunnel into the screenhouse, where it passes through a coarse screen and fine-mesh traveling screens before being pumped to the condenser or service water system. The water from these two systems is combined and released to the discharge canal which opens into Lake Ontario at the shoreline. The discharge canal is an open structure approximately 20 ft wide at the base with side slopes of 1:1 at lake entry. Average water depth in the canal is about 8 ft and a discharge velocity of 3.7 fps is typical. The 400,000 GPM flow is normally maintained at all power levels and its discharge velocity, which depends upon on lake elevation, is presented in Figure 1.4-27.

1.3 SYSTEM OPERATION

1.3.1 Circulating Water System

The waste heat released to Lake Ontario by the plant is about 4.0×10^9 BTU/HR at the 490 MWe rated output. The water used to remove heat from the main condensers is provided by a once-through circulating system designed to limit the temperature rise through the main condensers to a maximum of approximately 20F° at 100 percent of rated capacity. As presented in Figure 1.2-1, 381,000 GPM of the measured 400,000 GPM total circulating water flow passes through the condensers and 19,000 GPM flow through the service water system. A temperature increase of 20F° has been assumed across the service water system for calculations of waste heat rejection.

The 400,000 GPM circulating flow is normally maintained at all power levels except during periods of recirculation to prevent the accumulation of frazil ice on the intake structures. Retention time of condenser cooling water in the plant system is approximately eight minutes and no consumption or process contact of the water occurs.

1.3.2 Recirculation

During normal operating conditions, at rated thermal power, the temperature of the water that leaves the discharge canal is increased about 20F° above the temperature of withdrawal from Lake Ontario. During the period from mid-December through mid-April, a portion of the condenser discharge water

is recirculated to the forebay to prevent any ice accumulation on the screenhouse facilities. Ginna operating procedures state that condenser water inlet temperature should be maintained at no more than 40°F maximum by use of the recirculation gate during the winter months. Discharge flow rates versus temperature excess during the recirculation mode are presented in Figure 1.4-28. Under such conditions of maximum recirculation, the temperature of the discharge water to Lake Ontario would be increased 28F° above inlet water temperatures. Recirculation has the effect of lowering the flow rate while raising the discharge excess temperature. Plume development with reference to winter recirculation is discussed in section 1.4.2.4.

1.3.3 Biocide Treatment

Sodium hypochlorite is intermittently added to the intake water at the forebay to inhibit biological growths and maintain heat transfer efficiency in the main condenser and house service water systems. Total residual chlorine is continuously monitored during chlorination periods.

In January 1977, chlorination procedures at Ginna have been reduced to one 30 minute period per day five times per week in an effort to keep chlorine discharges as low as practicable. The facility is operating in compliance with its NPDES effluent limitation of 0.5 mg/l free available chlorine and maximum value of 45.4 kg/day (100 lbs/day).

1.3.4 Reactor Shutdown

Scheduled shutdowns for refueling and maintenance generally occur once a year for about a six week period. It is expected that the refueling outage would normally occur during the Spring or Fall when electrical system demands are at a minimum and not during the period December through March, except as required by New York Power Pool Planning (NYPP). Coordination of planned shutdowns with NYPP is required so that an acceptable state power reserve is maintained.

Any changes in reactor power during operation will cause time-varying temperature behavior in the thermal plume. A normal startup or shutdown would typically result in finer incremental temperature changes in the circulating water discharge than an emergency shutdown. The severest impact would result from the simultaneous occurrence of the following conditions:

(1) full-power operation in winter,
(2) maximum recirculation,
(3) instantaneous decrease from full-power operation to zero-power, and
(4) continued operation of the main circulating water pumps.

The temperature drop of the discharge water associated with rapid outage would be most severe during the first minute (about 17°F). The average number of unscheduled shutdowns per year for the Ginna unit is 10 based upon a 5 year operation period.

LIST OF FIGURES (continued)

LIST OF FIGURES (continued)

CHAPTER 1.0

THERMAL PLUME CHARACTERISTICS

1.1 PLANT DESCRIPTION

The Ginna Nuclear Power Plant is located on Lake Ontario in the northwest corner of Wayne County, N.Y. This location, on the south shore of Lake Ontario, is about 20 miles ENE of Rochester, N.Y. and 45 miles WSW of Oswego, N.Y. Figure 1.1-1 shows the counties and the larger cities and towns within 50 miles of the site. The nearest planned and existing nuclear facilities are located at the Sterling site (about 34 miles away) and Nine Mile Point Units (about 49 miles away), respectively.

Rochester Gas and Electric Corporation (RG&E) obtained its provisional license on September 19, 1969 to operate Ginna at 1300 megawatts thermal (MWt). The AEC Directorate of Licensing amended this provisional operating license to RG&E on March 1, 1972 to allow operation at power levels up to 1520 MWt. A pressurized-water reactor (PWR) is used to produce this thermal power level. A steam turbine-generator uses this heat to provide 490 MWe (net) of electrical power capacity.

The plant consists of a closed-cycle, pressurized, light-water-moderated nuclear steam-supply system, a turbine-condenser system, and auxiliary equipment. Figure 1.1-2 is a simplified flow diagram of the steam-electric system. After passing through the turbines, spent steam is condensed by once-through cooling with water from Lake Ontario. At full design power, the plant removes water from Lake Ontario at the rate of 400,000 GPM and heats it to a temperature 20F° above ambient lake temperature before returning it to the lake as a shoreline surface discharge.

1.2 HEAT DISSIPATION SYSTEM DESCRIPTION

Heat-removal facilities for normal operations consists of a conventional once-through system with cooling water being withdrawn from and returned to the same waterbody. The intake-discharge facilities are designed to provide the water requirements for the circulating water system and the house service water system. The total flow of circulating water through these systems under normal operating conditions is about 400,000 GPM (891.2 CFS). Figure 1.2-1 is a flow diagram of these once-through systems. Lake Ontario is the

source and recipient of the circulating water which is withdrawn through a submerged octagonal intake structure that lies some 3100 ft offshore in about 35 ft of water. Figure 1.2-2 is a perspective drawing of the intake structure, screenhouse and discharge canal. Intake water flows by gravity through a 10 ft diameter concrete-lined tunnel into the screenhouse, where it passes through a coarse screen and fine-mesh traveling screens before being pumped to the condenser or service water system. The water from these two systems is combined and released to the discharge canal which opens into Lake Ontario at the shoreline. The discharge canal is an open structure approximately 20 ft wide at the base with side slopes of 1:1 at lake entry. Average water depth in the canal is about 8 ft and a discharge velocity of 3.7 fps is typical. The 400,000 GPM flow is normally maintained at all power levels and its discharge velocity, which depends upon on lake elevation, is presented in Figure 1.4-27.

1.3 SYSTEM OPERATION

1.3.1 Circulating Water System

The waste heat released to Lake Ontario by the plant is about 4.0×10^9 BTU/HR at the 490 MWe rated output. The water used to remove heat from the main condensers is provided by a once-through circulating system designed to limit the temperature rise through the main condensers to a maximum of approximately 20F° at 100 percent of rated capacity. As presented in Figure 1.2-1, 381,000 GPM of the measured 400,000 GPM total circulating water flow passes through the condensers and 19,000 GPM flow through the service water system. A temperature increase of 20F° has been assumed across the service water system for calculations of waste heat rejection.

The 400,000 GPM circulating flow is normally maintained at all power levels except during periods of recirculation to prevent the accumulation of frazil ice on the intake structures. Retention time of condenser cooling water in the plant system is approximately eight minutes and no consumption or process contact of the water occurs.

1.3.2 Recirculation

During normal operating conditions, at rated thermal power, the temperature of the water that leaves the discharge canal is increased about 20F° above the temperature of withdrawal from Lake Ontario. During the period from mid-December through mid-April, a portion of the condenser discharge water

is recirculated to the forebay to prevent any ice accumulation on the screenhouse facilities. Ginna operating procedures state that condenser water inlet temperature should be maintained at no more than 40°F maximum by use of the recirculation gate during the winter months. Discharge flow rates versus temperature excess during the recirculation mode are presented in Figure 1.4-28. Under such conditions of maximum recirculation, the temperature of the discharge water to Lake Ontario would be increased 28F° above inlet water temperatures. Recirculation has the effect of lowering the flow rate while raising the discharge excess temperature. Plume development with reference to winter recirculation is discussed in section 1.4.2.4.

1.3.3 Biocide Treatment

Sodium hypochlorite is intermittently added to the intake water at the forebay to inhibit biological growths and maintain heat transfer efficiency in the main condenser and house service water systems. Total residual chlorine is continuously monitored during chlorination periods.

In January 1977, chlorination procedures at Ginna have been reduced to one 30 minute period per day five times per week in an effort to keep chlorine discharges as low as practicable. The facility is operating in compliance with its NPDES effluent limitation of 0.5 mg/l free available chlorine and maximum value of 45.4 kg/day (100 lbs/day).

1.3.4 Reactor Shutdown

Scheduled shutdowns for refueling and maintenance generally occur once a year for about a six week period. It is expected that the refueling outage would normally occur during the Spring or Fall when electrical system demands are at a minimum and not during the period December through March, except as required by New York Power Pool Planning (NYPP). Coordination of planned shutdowns with NYPP is required so that an acceptable state power reserve is maintained.

Any changes in reactor power during operation will cause time-varying temperature behavior in the thermal plume. A normal startup or shutdown would typically result in finer incremental temperature changes in the circulating water discharge than an emergency shutdown. The severest impact would result from the simultaneous occurrence of the following conditions:

(1) full-power operation in winter,
(2) maximum recirculation,
(3) instantaneous decrease from full-power operation to zero-power, and
(4) continued operation of the main circulating water pumps.

The temperature drop of the discharge water associated with rapid outage would be most severe during the first minute (about 17°F). The average number of unscheduled shutdowns per year for the Ginna unit is 10 based upon a 5 year operation period.

LOCATION OF THE GINNA NUCLEAR POWER PLANT

RGE ROCHESTER GAS AND ELECTRIC

Figure 1.1-1

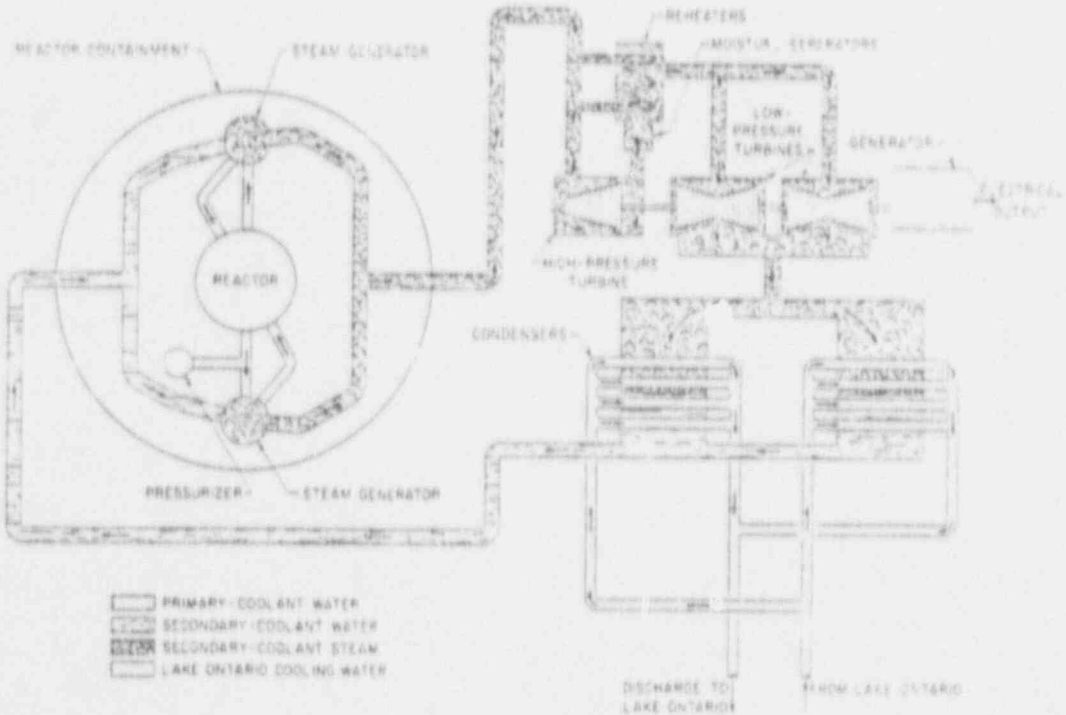

SIMPLIFIED FLOW DIAGRAM OF THE STEAM-ELECTRIC SYSTEM OF THE GINNA NUCLEAR POWER PLANT

ROCHESTER GAS AND ELECTRIC

Figure 1.1-2

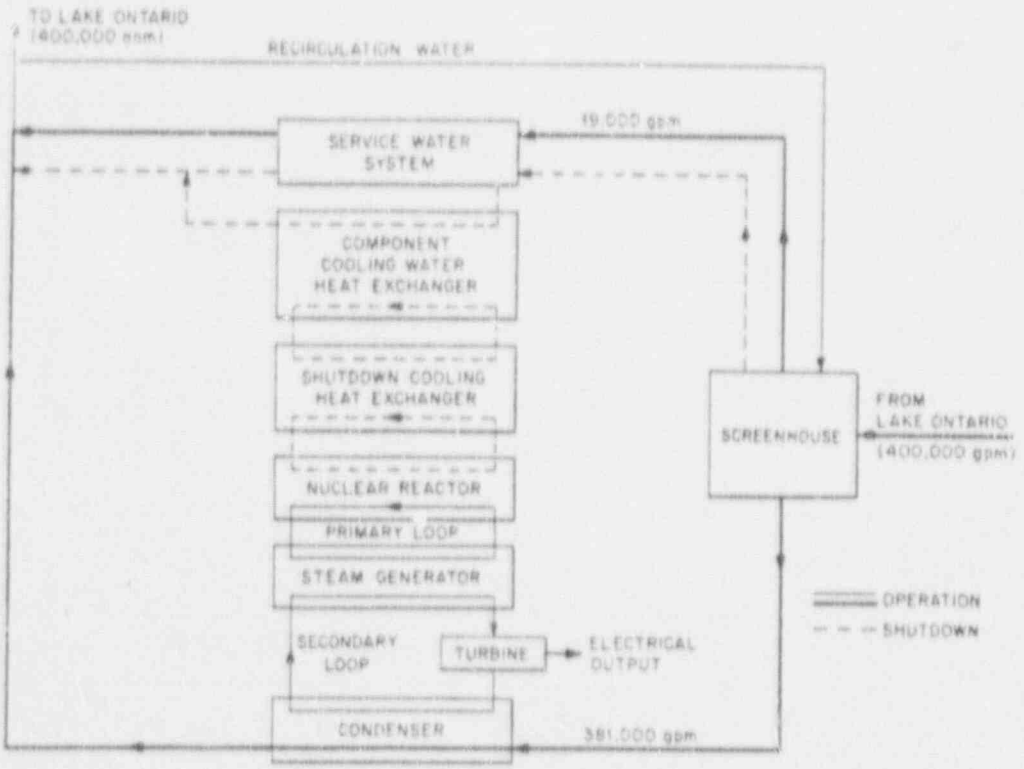

SIMPLIFIED FLOW DIAGRAM OF THE CONDENSER AND SERVICE-WATER SYSTEMS OF THE GINNA NUCLEAR POWER PLANT.

RGE ROCHESTER GAS AND ELECTRIC

Figure 1.2-1

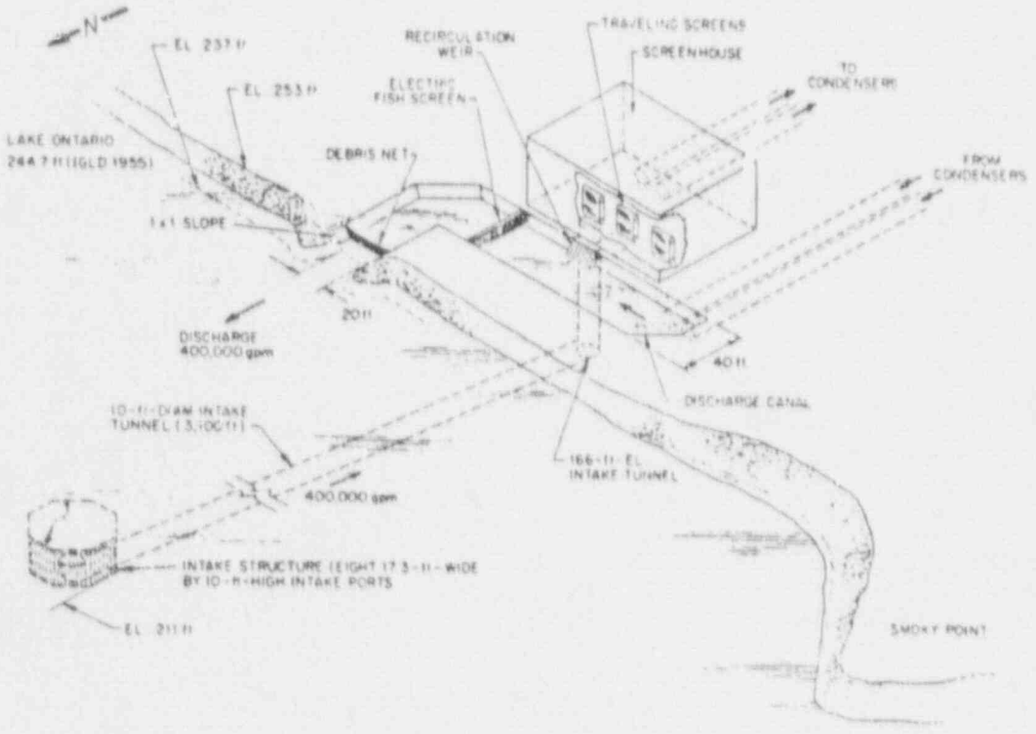

PERSPECTIVE DRAWING OF THE INTAKE STRUCTURE, SCREEN-HOUSE, AND DISCHARGE CANAL OF THE GINNA NUCLEAR POWER PLANT

RGE ROCHESTER GAS AND ELECTRIC

Figure 1.2-2

1.4 THERMAL PLUME MODEL AND CHARACTERISTICS

1.4.1 MATHEMATICAL MODEL USED

1.4.1.1 Discussion of Model

1.4.1.1.1 Introduction

1.4.1.1.1.1 Problem Description

When a stream of warm water is released from an open channel into a large body of water, the warmer effluent mixes with the cooler ambient water, resulting in spreading and cooling of the discharge. The area in the receiving body where the discharge can be sensed is referred to as the thermal plume. The plume can be thought of as being comprised of four basic regions: the core region, in which the initial jet effect of the discharge results in a mixing of the plume with the ambient water but in which the temperature and velocity of the plume centerline remain essentially constant; the entrainment region, in which the turbulent shear forces caused by the velocity difference between the plume and ambient result in the mixing of cooler water with the discharge plume while the buoyancy of the warmer water tends to cause the plume to rise; the stable region, in which the plume continues to spread due to the buoyant rising of the warm water but in which the rate of entrainment is inhibited by the low plume velocity and the high density stratification between the plume and ambient; and the far field, in which the plume surface area is large enough to allow significant heat transfer from the lake to the atmosphere. This discussion is intended to concentrate on the near field portion of the plume, which essentially encompasses the first three regions.

The temperature distribution within these regions are influenced by many variables such as location within the plume, discharge channel geometry, discharge water temperature and flow rate, ambient water temperature, elevation, turbulence level, and velocity, lake shore and bottom configuration, and atmospheric conditions.

1.4.1.1.1.2 Possible Solution Methods

A number of theoretical models exist to describe a surface jet discharge. For example, Motz and Benedict[1] formulated a two dimensional model. However, the two dimensionality of the model results in neglect of jet spreading due to buoyancy. Stolzenbach and Harleman[2] and Shirazi and Davis[3] have formulated three dimensional models for deep receiving waters. However, these

formulations cannot be used past the entrainment region due to their underlying assumption that jet momentum is much greater than ambient momentum. Also, their predictions are not accurate for shallow receiving waters. When one considers the complexity of the thermal plume and the many variables which affect it, it is not surprising that a general theoretical model does not exist which will give acceptable predictions of the thermal distribution in a shallow receiving basin, such as the nearshore region of Lake Ontario, due to a surface jet discharge of heated water.

An alternative to the use of a theoretical model as the chief predictive tool in determining the effects of the Ginna discharge is an empirical model. Examples of empirical models are those of Pritchard,[4] Asbury and Frigo,[5] and Shirazi.[6] Such models have the advantage of being based upon actual field measurements of surface jet discharges, thereby implicitly accounting for all of the governing mechanisms. However, their disadvantage is related to their advantage. That is, since all of the mechanisms governing plume behavior are implicitly accounted for, extrapolation of these formulations to sites not similar to those used to derive the formulations is not good practice. This is because the relative magnitude of the various mechanisms may be entirely different at different sites.

It should be clear from the above that the best method of predicting the effects of a discharge is to use a formulation based upon direct field measurements. In this light, extensive data are available for the R.E.Ginna Nuclear Power Plant surface jet discharge. Therefore, an empirical model based upon these extensive field measurements will be developed. This model will then be used to assess the effects of the Ginna discharge.

1.4.1.1.1.3 Other Empirical Models

A number of empirical studies of surface jet discharges are available in the literature. Pritchard[4] used data from a number of sites along the Great Lakes to arrive at an algorithm for drawing surface isotherms. This model, however, is quite arbitrary in that the chief dependent variables are channel width and discharge temperature. No functional dependence is included for such basic factors as discharge flow, discharge Froude number, etc. The model is applicable to the original data base because the governing factors vary over a fairly narrow range. The plants studied were relatively low capacity fossil fired units with low velocity discharges. The use of this model for the Ginna plant would be inappropriate.

Asbury and Frigo[5] also studied various Great Lakes sites to arrive at a relation between dimensionless excess centerline

temperature, and the ratio of isotherm area to discharge flow, I/Q_o . It is obvious, however, that the latter parameter has the dimensions of inverse velocity. If two data sources have different length scales, the same temperature rise, and equivalent Froude numbers, the latter being required if the near field jet behavior is going to be the same at the two sites, then the ratio of their isotherm areas would be proportional to the square of the ratio of their length scales while the ratio of their flows must be proportional to the 2.5 power of the length scale ratio. Therefore, it would be incorrect to use the parameter I/Q_o for data sources other than those from which the relationship was derived.

Shirazi[6] investigated the centerline temperature excess and plume half width of a number of data sources. He took a purely statistical approach and assumed that

$$\frac{\Delta T_c}{\Delta T_o} \quad \text{and} \quad \frac{r_h}{h_o} = a' \left(\frac{s}{h_o}\right)^{b'} R'^{c'} F^{d'} A^{e'} a_c^{f'} \qquad (1)$$

where:

ΔT_c = centerline temperature excess, ^oF

ΔT_o = discharge temperature excess, ^oF

r_h = plume half width, ft

h_o = discharge depth, ft

s = distance along plume trajectory, ft

R' = ambient velocity/discharge velocity = U_a/U_o

F = densimetric Froude number = $U_o \Big/ \sqrt{g h_o \frac{(\rho_a - \rho_o)}{\rho_a}}$

A = aspect ratio = W/h_o

a_c = angle between discharge and ambient velocities, radians

U_a = ambient velocity, ft/sec

U_o = discharge velocity, ft/sec

g = gravitational acceleration, ft/sec^2

W = discharge channel width, ft

ρ_a = ambient density, lb/ft^3

ρ_o = discharge density, lb/ft^3

and a',b',c',d',e',f' = correlation constants which are different for $\frac{\Delta T_c}{\Delta T_o}$ and $\frac{r_h}{h_o}$

Stefan, et al [7] investigated plume effects within the core region and slightly beyond and found that

$$\frac{s}{h_o} = (a'-b'T)^{c'} \quad A^{d'-e'T} \quad \exp(-f'R')\left[1+\frac{g'F-h'}{\exp(i'F)}\right] \qquad (2)$$

where: $T = \Delta T_c/\Delta T_o$ = dimensionless centerline temperature excess

and g',h',i' = correlation constants

resulted in a good fit to the data for $1.0 \leq A \leq 9.6$, $0 \leq R' \leq 0.41$, $2.0 \leq F \leq 15$, and $0.8 \leq T \leq 0.98$.

1.4.1.1.2 Analytical Discussion

1.4.1.1.2.1 Describing Parameters

The effects of a surface jet discharge are influenced by many variables. In the near field these variables can be reduced to the dimensionless parameters F,A,R',K (where $K = k/\rho_a C_p U_o$ where k = surface heat transfer coefficient, Btu/ft^2 - ^oF - sec and C_p = specific heat of water, Btu/lb-^oF), and α_c for a deep receiving water body. For a shallow receiving water body, the effect of lateral and bottom boundaries must also be considered. Ambient turbulence is considered to have secondary importance within the near field.(2)

The heat loss parameter, K, can always be neglected in the near field for practical purposes.(8) This can best be illustrated by a sample calculation. Using Figure 1.4-29 which shows the expected spring surface isotherms, and taking a value of k = 92 Btu/ft^2 - ^oF - day, an average value for Lake Ontario,(9) the heat lost through the surface of the plume to the atmosphere was calculated. It was found that less than 3 percent of the heat rejected to the lake by the plant was lost to the atmosphere within the 2^{o}F isotherm.

R' and its associated parameter α_c have not been measured at Ginna. This is not considered to be a serious deficiency in this case. A surface jet in the presence of a crossflowing ambient will exhibit a distortion of the lateral temperature profiles. However, if R' is much less than one, the effects of the crossflow on the plume temperature distribution will be small. The major effect of the crossflow will be a gradual bending of the jet trajectory.(8) At Ginna the discharge velocities are in the range of 3-5 ft/sec., an order of magnitude larger than the currents normally occurring on Lake Ontario. Therefore, the effects of lake currents are expected to be small. It is important to realize that if lake velocities larger than normally expected were to occur, the plume would exhibit greatly increased entrainment rates and, therefore, a much greater rate of temperature decay.(8,10) Hence, at large lake velocities where the crossflow becomes important, its effect is to significantly decrease the size of the thermal plume. On these bases, the parameters R' and α_c are not considered further.

A linear scaling factor must be defined so that the plume parameters s, r_h, and I, the isotherm area, can be described in dimensionless form. Shirazi(6) and Stefan, et al(7) used the discharge depth, h_o. Inspection of their general functional forms, equations 1 and 2, shows that the discharge flow, $Q_o = U_o a$, where a = cross section

area of discharge flow, is accounted for through the use of the variables F,A, and the scale factor h_o. However, a better choice of length scale would be $\sqrt{a/2}$. Use of this factor in the formulation will reduce the dependence of plume behavior on the aspect ratio,[2] the aspect ratio no longer being necessary to define the size of the discharge.

1.4.1.1.2.2 Centerline Temperature Excess

As described in Section 1.4.1.1.1.3, Shirazi[6] described the dimensionless centerline temperature excess, T, as the product of the describing parameters raised to constant powers, as shown in equation 1. For a specific set of lake and discharge conditions, this equation form reduces to a straight line when log T is plotted against $\log(s/h_o)$. Figure 1.4-1, which describes the centerline temperature decay at Ginna based on some early field measurements, is such a plot. Note that the curves defining centerline temperature decay are not straight lines. Rather than h_o, $\sqrt{a/2}$ has been used as the scale factor. For a specific set of conditions, use of h_o would result in a translation of the curves without changing their shape or slope. As is obvious, the functional form used by Shirazi to describe the dependence of T on the distance along the plume trajectory, X, is not appropriate for Ginna.

The form used by Stefan, et al[7] was also considered. Although this formulation was derived only for $0.8 \leq T \leq 0.98$, it was thought that the same functional representation, equation 2, might be applicable to the entire range of temperature excess. As discussed previously, the value of R' can be considered to be essentially zero for this study. Therefore, equation 2 becomes:

$$\frac{s}{h_o} = (a'-b'T)^{c'} \; A^{d'-e'T} \left[1+\frac{g'F-h'}{\exp\,(i'F)}\right] \qquad (3)$$

Using $\sqrt{a/2}$ instead of h_o as the linear scale factor, equation 3 becomes

$$\chi = \frac{s}{\sqrt{a/2}} = (a'-b'T)^{c'} \; A^{d'-e'T} \left[1+\frac{g'F-h'}{\exp\,(i'F)}\right] \qquad (4)$$

where: χ = dimensionless distance along jet trajectory
and a',b',c',d',e',g',h', and i' may have different values than in equation 3.

The function describing the effects of Froude number, the term in brackets in equation 4, was investigated. The values of g',h', and i' found by Stefan, et al[7] were 0.5, 1.5, and 0.4 respectively. However, this Froude number function is very difficult to work with statistically in that it cannot be linearized. Therefore, a new function is sought which would reproduce the basic characteristics of Stefan's function but would be easier to manipulate. The first attempt would obviously be Shirazi's function,

$$f(F) = a'F^{b'} \tag{5}$$

where: f(F) = functional dependence of T on F.

However, as is quickly obvious, equation 5 is a monotonic function, whereas Stefan's function,

$$f(F) = 1 + \frac{g'F-h'}{\exp\ (i'F)} \tag{6}$$

has an extremum located at,

$$F = \frac{i'h'+g'}{i'g'} \tag{7}$$

The required functional form of f(F) must, therefore, also have an extremum. A possible function can be deduced from Shirazi. If equation 5 is expressed in a slightly different form,

$$f(F) = \exp\ (a''+b'\ln F) \tag{8}$$

where: a" is a new correlation constant,
then an extension of this can be postulated as,

$$f(F) = \exp\left[\alpha'+\beta'\ln F+\gamma'(\ln\ F)^2\right] \tag{9}$$

where: α', β', and γ' are new correlation constants.

Using the values of g', h', and i' found by Stefan, the method of least squares, which will be explained in Section 1.4.1.1.4, was used to find the best fit of equations 5 and 9 with equation 6 for the range of Froude numbers spanned by the Ginna data. As will be shown in Section 1.4.1.1.3, this range of F is from approximately 3 to 13. Figure 1.4-2 graphically shows the comparison between these functions. As expected, equation 5 is a poor substitute for equation 6, whereas equation 9 mimics the characteristics of equation 6 quite well.

If equation 9 is substituted for equation 6 in equation 4 then the equation describing the centerline temperature excess becomes,

$$\chi = (a'-b'T)^{c'} \quad A^{d'-e'T} \exp\left[\alpha' + \beta' \ln F + \gamma' (\ln F)^2\right] \qquad (10)$$

The use of aspect ratio as one of the describing parameters in equation 10 must be examined further in light of the present study. The aspect ratio is defined as,

$$A = W/h_o \qquad (11)$$

However, the Ginna data is derived from a single discharge with a constant channel width, W. On the other hand, the discharge depth, h_o, varies directly with the lake elevation. Therefore, any changes in aspect ratio are directly related only to changes in lake elevation, or lake depth. If A were used to describe the thermal distribution at Ginna, it would not be known whether plume charges were due to variation in lake elevation or aspect ratio. In a shallow body of water, changes in lake water depth may result in changes in thermal plume behavior due to a variation in the characteristics of plume interference with the lake bottom. The phenomenon of plume interference with the lake bottom does not occur in deep water bodies. The latter case was the one investigated by Stefan, et al,[7] and therefore the use of A as a describing parameter did not lead to any uncertainty in model interpretation. In this case, however, model interpretation will be aided by determining whether the variation in lake water depth or aspect ratio is the controlling mechanism. Model results, of course, depend only on knowing the effect of lake elevation on the plume and not on knowing which mechanism is controlling.

As described previously in this section, the use of $\sqrt{a/2}$ as the scale factor for length, rather than h_o, as used by Stefan, reduces the dependence of the plume description on the aspect ratio. Stolzenbach, et al[12] found that the governing equations

outside of the core region in a deep receiving water body are only dependent upon a modified densimetric Froude number, F', where,

$$F' = FA^{-\frac{1}{4}} \tag{12}$$

This indicates that plume characteristics are insensitive to changes in aspect ratio as compared with changes in Froude number. Since the effects of aspect ratio variations are known to be small, a significant effect of lake elevation on the plume can only be interpreted as signifying that lake depth variations are the controlling mechanism.

The parameter describing lake water depth can be taken as lake surface elevation minus an effective lake bottom elevation which would result in a similar thermal distribution as the sloping bottom at Ginna. In order to reduce this parameter to dimensionless form, the length scale factor, $\sqrt{a/2}$, might be considered. However, since changes in channel cross section area, a, are due solely to changes in lake water depth, the use of $\sqrt{a/2}$ as a scale factor would effectively be the same thing as considering the square root of the lake depth as the dimensionless parameter. This, of course, is no longer dimensionless, having the dimension of $ft^{\frac{1}{2}}$. A better choice as scale factor would be the average lake depth. This value is independent of the instantaneous lake depth. Therefore, in place of aspect ratio, a dimensionless lake depth is used, which is defined as,

$$D = \frac{E-b}{\bar{E}-b} \tag{13}$$

where: E = lake surface elevation, ft
b = effective lake bottom elevation, ft
$\bar{E}$ = average lake surface elevation, ft
D = dimensionless lake depth

The use of D rather than A as a describing parameter leaves in question the appropriate functional form to be used in describing the centerline excess temperature of the plume. The functional form of the aspect ratio used by Shirazi[6] was,

$$f(A) = A^{e'} \tag{14}$$

where f(A) = functional dependence of T on A. Stefan, et al[7] used,

$$f(A) = A^{d'-e'T} \qquad (15)$$

The lake depth, or plume bottom interference, will have a varying effect along the length of a thermal plume. Initially, the plume would not interact significantly with the bottom. As the water is transported further from the discharge, turbulent shears induced by the discharge jet momentum would tend to deepen the plume, thereby resulting in greater bottom interference. As the discharge momentum was dissipated, buoyant forces would cause the plume bottom to rise off the lake bottom. Therefore, the functional form describing the dependence must possess the characteristic of an extremum at some point between 0 and 1. An extension of equations 14 and 15 is of the form,

$$f(D) = D^{n_1 + n_2(T-1) + n_3(T-1)^2} \qquad (16)$$

where: $f(D)$ = functional dependence of T on D
n_1, n_2, n_3 = correlation constants

and T-1 is used in place of T so that the value at the end of the core region, T=1, is readily apparent. The use of T-1 rather than T does not change the function but does change the correlation constants.

Substituting equation 16 for 15 in equation 10 results in,

$$\chi = (a'-b'T)^{c'} D^{n_1+n_2(T-1)+n_3(T-1)^2} \exp\left[a' + \beta' \ln F + \gamma' (\ln F)^2\right] \qquad (17)$$

Equation 17 was investigated with respect to the major temperature dependence,

$$f(T) = (a'-b'T)^{c'} \qquad (18)$$

where: $f(T)$ describes the major interdependence of T and χ. This functional form, although adequately describing the shape of the Ginna data found in Figure 1.4-1, is statistically very difficult to work with due to the impossibility of expressing it in linear form. Also, as described in Section 1.4.1.1.3, less than 1% of the Ginna data has dimensionless excess centerline temperatures greater than 0.8, the lower limit of the range of Stefan's data. Equation 18 was used to fit sample data for $T<0.8$. It was found that $b' > a'$. Therefore, $f(T)$ in equation 18 is negative for T=1. This, of course, is physically unrealistic. The dual problems of physical realism and difficulty of manipulation required a different function than that given in equation 18.

In earlier parts of this section, the inadequacy of Shirazi's[6] functional form, which can be derived from equation 1 as,

$$f(T) = a'T^{b'} \tag{19}$$

where a' and b' are the inverses of the correlation constants indicated in equation 1, was discussed. Equation 18, on the other hand, does provide a clue to a convenient and realistic function. Rather than using a'-b'T as the base for an exponent c', c' was used as a base for the exponent a'-b'T. This can be expressed as,

$$f(T) = c'^{a'-b'T} \tag{20}$$

Equation 20 can be transformed to,

$$f(T) = \exp\left[\phi' + \psi'(T-1)\right] \tag{21}$$

where: $\phi' = (a'-b')\ln c'$ = new correlation constant
$\psi' = -b' \ln c'$ = new correlation constant

and a',b' and c' are the values appropriate for equation 20. Note that one less correlation constant is necessary for the description f(T) in the form of equation 21 than is required in the form of equation 20. As in equation 18, T-1 is used rather than T so that the value of f(T) at the end of the core region is readily calculable.

Unlike equation 18, equation 21 has the advantage of always being positive at the end of the core region . This is readily apparent by substituting T=1, the definition of the end of the core region, into equation 21. The result is

$$f(T) = e^{\phi'} \quad \text{at} \quad T=1 \tag{21a}$$

This function is greater than zero for any value of ϕ'.

Equation 21 has the additional advantage of being readily expanded to include higher powers of T-1. For example,

$$f(T) = \exp\left[\phi'' + \psi(T-1) + \theta(T-1)^2\right] \tag{22}$$

where: ϕ'', ψ, and θ are correlation constants, might be used to improve the fit of equation 21 to the data.

For illustration purposes, the method of least squares, which will be explained in Section 1.4.1.1.3, was used to determine

the constants of equations 21 and 22 so as to provide the best fit to the worst case, surface curve of Figure 1.4-1, which shows the actual trend of the Ginna data. Figure 1.4-3, is a graphical depiction of the results. It is seen that both equations 21 and 22 are good representations of the data, but, as expected, equation 22 is a slightly better fit.

Replacing equation 18 with equation 22 in equation 17 results in,

$$\chi = \exp\left[\phi'' + \psi(T-1) + \theta(T-1)^2\right] D^{n_1+n_2(T-1)+n_3(T-1)^2} \quad (23)$$

$$\times \exp\left[\alpha' + \beta' \ln F + \gamma' (\ln F)^2\right]$$

Equation 23 can also be expressed as,

$$\chi = \exp\left[\phi + \psi(T-1) + \theta(T-1)^2\right] D^{n_1+n_2(T-1)+n_3(T-1)^2} \quad (24)$$

$$\times \exp\left[\beta' \ln F + \gamma' (\ln F)^2\right]$$

where $\phi = \phi'' + \alpha'$ of equation 23 = new correlation constant.

Equation 24 represents the general form used in this study to determine the dependence of temperature excess along the plume centerline on lake elevation and Froude number. The latter depends on discharge velocity, which, for a constant discharge flow rate and channel width such as exists at Ginna, depends only upon lake elevation, discharge flow depth, which also depends only on lake elevation at Ginna, and $(\rho_a - \rho_o)/\rho_a$, which, for a constant excess discharge temperature, depends only on lake temperature. Therefore, for a constant discharge excess temperature, equation 24 actually shows the effects of varying lake elevation and lake temperature on the centerline excess temperature of the plume.

1.4.1.1.2.3 Plume Half Width

The plume half width, r_h, is a convenient parameter for describing the manner in which the plume spreads. Shirazi[6] assumed that the same functional form describes plume half width and centerline temperature excess. However, Figure 1.4-1 indicates that the functional form describing the dependence of r_h on s is quite different than the form of T versus s indicated in equation 21 or 22.

Engelund and Pederson[13] developed a semi-empirical model to describe the temperature distribution near the discharge point

of a high Froude number surface jet discharging into a deep, stagnant water body. Edinger, et al [14] reduced the work of Engelund and Pederson into two possible surface distributions of excess temperature,

$$\frac{\Delta T}{\Delta T_o} = \frac{\Delta T_c}{\Delta T_o} \exp\left[-\frac{14}{9} F^2 \left(\frac{r}{\sqrt{a/2}}\right)^2 \chi^{-14/3}\right] \quad (25)$$

and

$$\frac{\Delta T}{\Delta T_o} = \frac{\Delta T_c}{\Delta T_o}\left[1+\frac{14}{9} F^2 \left(\frac{r}{\sqrt{a/2}}\right)^2 \chi^{-14/3}\right]^{-1} \quad (26)$$

where: r = plume width at excess temperature ΔT and dimensionless longitudinal distance χ, ft

and ΔT = excess temperature at location (χ, r), ^oF

If ΔT is taken as one half ΔT_c, then $r=r_h$ in equation 25 and 26 by definition.

If equations 25 and 26 are then solved for r_h the results are,

$$r_{0.5} = 0.67\ \chi^{7/3} F^{-1} \quad (27)$$

and $$r_{0.5} = 0.80\ \chi^{7/3} F^{-1} \quad (28)$$

where $r_{0.5} = r_h / \sqrt{a/2}$ = dimensionless plume half width. Equations 27 and 28 correspond to equations 25 and 26 respectively.

Equations 27 and 28 can be seen to be similar in form to Shirazi's function; that is,

$$r_{0.5} = a' \chi^{b'} F^{d'} \quad (29)$$

where a',b' and d' are correlation constants different than those of equation 1.

Equation 29 differs from equation 1 in that no functional dependence is present for R, α', and A. R and α' are not included because Engelund and Pederson considered a stagnant receiving water. As discussed near the beginning of this section, $r_{0.5}$ may be taken as independent of R and α' for the present study. That is, from

the standpoint of plume dilution at Ginna, Lake Ontario may be considered as a stagnant body of water.

The aspect ratio, A, was thoroughly discussed in Section 1.4.1.1.2.2. It was shown that D, the dimensionless lake depth, was a better variable to consider than A for a shallow receiving water body such as Lake Ontario at the Ginna site. However, experimental data[2,8] has shown that the plume half width does not depend upon the receiving water depth. Therefore, it is expected that $r_{0.5}$ will depend only on X and F in a manner similar to equation 29.

Note that the plume half width curves of Figure 1.4-1 would be straight lines if equation 29 were a proper description of the Ginna data. Since they are not, the functional form of equation 29 is extended in a similar manner to the extension of equation 8 into equation 9. The resulting equation, which includes a possible lake depth dependence is,

$$r_{0.5}=\exp\left[\alpha+\beta\ln X+\gamma(\ln X)^2+\delta\ln F+\epsilon(\ln F)^2+\zeta\ln D\right] \qquad (30)$$

Note that the functional form of D is not as complicated as the form for X and F. This is because, as explained previously, $r_{0.5}$ is not expected to depend on D. If the data verifies this, the last term in equation 30 will be dropped. If the analysis of the Ginna data shows otherwise, the functional form of D can easily be expanded into a form similar to either equation 9 or equation 16.

1.4.1.1.2.4 Lateral Distribution

The lateral excess temperature distribution in a surface jet discharge plume is usually assumed to be Gaussian in form.[3,6,8,11,14] In those cases where other forms are used,[2,13] the resulting distribution does not vary greatly from that which would be given by a Gaussian relationship.

The lateral temperature distribution at Ginna will therefore be expressed as,

$$T_m = n\exp\left[-p(r/r_h)^2\right] \qquad (31)$$

where: $T_m = \Delta T/\Delta T_c$ = dimensionless lateral temperature at r

n and p = constants

and r and r_h are as defined previously. Outside of the core

region, r must be 0 when $T_m = 1$. Also, by definition, r must equal r_h when $T_m = 0.5$. Substituting these conditions into equation 31, and solving for n and p results in,

$$n = 1 \qquad (32)$$

$$p = \ln 2 = 0.693$$

The use of equations 31 and 32 does not allow for any variation of the postulated distribution which may be inherent in the Ginna data. However, data variations can be accounted for by assuming that separate distributions be calculated for the ranges $0.5 \leq T_m \leq 1$ and $T_m \leq 0.5$. If equation 31 is used for both ranges, then it has been shown previously that equations 32 must hold for $0.5 \leq T_m \leq 1$. However, the distribution for $T_m \leq 0.5$ requires only that $r = r_h$ when $T_m = 0.5$. Substituting this criterion into equation 31 and solving for n in terms of p results in,

$$n = 0.5 \exp(p) \qquad (33)$$

If $p = \ln 2$ then equation 33 is equivalent to equation 32.

The lateral distribution for this study is therefore taken as equations 31 and 33. The equation set 32 is noted as a special case of equation 33.

1.4.1.1.3 Data Description

1.4.1.1.3.1 Data Collection

Rochester Gas and Electric Corporation has an extensive field survey program for collecting lake temperature data in the vicinity of the Ginna discharge. During surveys, temperatures are continuously recorded from thermistors at four different depths along a grid pattern which is traversed by boat. Figure 1.4-4 shows the survey transect locations, bearing lines, and nine site-alignment target locations. The boat follows the bearing lines, its passing a transect intersection being noted on a multichannel strip-chart recorder. A pass is also made between intersections 14 and 20 to determine the fine structure of the plume in the region near the discharge. Ambient temperatures are determined from offshore thermal measurements outside of the plume area. When no horizontal thermal gradient is measured, ambient temperature is considered to have been sampled. The measured data are converted into isotherm plots at each depth. The surveys are performed approximately monthly, except during winter months and periods of plant shutdown. See Table 1.4-10.

1.4.1.1.3.2 Data Range

The above described isotherm plots for the period from the middle of 1970 to the middle of 1975 served as the data source for this analysis. As described in Section 1.4.1.1.2, the temperature excess at various locations within the plume will be functions of F, the densimetric Froude number, and D, the dimensionless lake depth. The latter variable, however, depends only upon the lake elevation, E.

In order to determine the Froude number, the discharge temperature, ambient temperature, and lake level, or discharge depth, must be known. The former two variables are measured by RG&E. Lake levels were obtained from NOAA[15] records for the Rochester gaging station. The levels used were the daily means reported by NOAA for the dates of the thermal surveys. For consistency, Froude numbers were calculated using the ambient temperature at the lake surface. Table 1.4-2 lists the survey dates and their associated values of F and E. Figure 1.4-5 is a graphical interpretation of Table 1.4-2, each point representing one survey. The figure shows that, although F ranges from 2.87 to 12.88, most of the data lie between 3.5 and 10. The elevation data, in feet USGS, range from 244.90 to 249.25, with the major cluster lying between 245 and 247.

Two survey dates, 3/19/70 and 3/30/72, were available but were not used. The ambient water temperatures in these two cases were 33°F and 34°F, respectively. Due to the fact that water density reaches a maximum at 39.2°F, the thermal plume will sink below the lake surface rather than remain at the surface for low

excess temperatures. This plume behavior can not be described in the same way as buoyant plume behavior. Therefore, these two dates were not used as part of the data base for this study.

1.4.1.1.3.3 Surface Data Reduction

Once the describing parameters F and E were found for each date, the thermal plume behavior for the corresponding survey was characterized. This was done by examining the appropriate surface isotherm plot (the surface data were actually taken at a depth of 0.5 feet) and determining the plume centerline by drawing a smooth curve through the vertices of the isotherms. The plume centerline in the plane of the isotherms defined the s coordinate.

Centerline temperatures were read at values of s corresponding to isotherm vertices. Centerline excess temperatures were determined by subtracting the field measured lake ambient temperature. Plume half widths were found corresponding to the s coordinates of isotherm vertices whose excess temperatures were multiples of 2. In this way, actual isotherm boundaries could be measured, thereby eliminating any need for determining half widths from interpolated values. The centerline temperature excesses were then scaled to the discharge excess temperature, while s and r_h were normalized to $\sqrt{a/2}$. The resulting dimensionless values defined the temperature decay and spreading characteristics of the plume.

Table 1.4-3 is a reproduction of the computer printout giving the data obtained by the methods described above. In this table, DT=date, FR=densimetric Froude number, ELEV=lake elevation in ft USGS, NO.PTS(CL)=number of centerline excess temperature data points for that date, NO.PTS(RHALF)=number of half width data points for that date, X=dimensionless longitudinal distance, T=dimensionless centerline excess temperature, and RHALF=dimensionless plume half width. A value of RHALF=-0.0 indicates that the plume half width at the corresponding longitudinal distance was not reduced. The bottom of the table shows that 425 centerline excess temperature data points and 197 half width data points were reduced at the surface. Figures 1.4-6 and 1.4-7 show typical data for the dates 9/25/70 and 10/27/71 in the same graphical form as Figure 1.4-1.

1.4.1.1.3.4 Subsurface Data Reduction

Temperature surveys at Ginna show that the thermal plume rarely goes below 9 or 10 feet. Therefore, the temperature distribution at a depth of 6 feet was used to describe the subsurface thermal effects. The surface and 6 foot isotherms describe the three dimensional aspects of the thermal distribution at Ginna.

Subsurface temperatures over the 5 years of data were sampled at various depths. Therefore, lake depths of 6 feet ±13 inches were nominally identified as 6 foot data.

Some of the survey dates did not include subsurface isotherms within the indicated depth range. Others had to be neglected due to anomalies in the isotherm patterns. This left 32 of the 43 surveys to form the subsurface data base for this study. Table 1.4-2 shows the dates and depths of those surveys that were used to indicate the subsurface behavior of the plume. A dash in the Subsurface Isotherm Depth column indicates a survey that was not used as input to the model.

The subsurface isotherms were measured and reduced in exactly the same manner as the surface isotherms, except for the determination of ambient temperature. In order to achieve the most realistic analysis of the Ginna data, any vertical lake temperature stratification was accounted for by taking the ambient temperature as that indicated in the appropriate isotherm plot rather than that measured at the lake surface. Table 1.4-4 gives the data reduced in the manner described above. The headings for this table are the same as those given for Table 1.4-3, the surface data listing. 259 centerline excess temperature data points and 111 half width data points were reduced. Figures 1.4-8 and 1.4-9 show typical plots of the data for 5/1/70 and 10/1/73.

1.4.1.1.4 Statistical Methods and Resulting Equations

1.4.1.1.4.1 Statistical Methods

In order to mathematically describe the Ginna data, a relation must be established between the data and the describing mathematical expressions. An often used method is the method of least squares.

The criterion describing the relationship between the data and the describing mathematical expression is,

$$\bar{S} = \sum_{i=1}^{m} \bar{e}_i^2 \quad \text{must be a minimum,} \tag{34}$$

where m = number of data points

$\bar{e}_i$ = difference between the i^{th} data point and the value of the mathematical expression at that point; that is, the error of the mathematical expression at data point i

and $\bar{S}$ = sum of the squares of the errors.

This method determines the coefficients of the mathematical expression such that the sum of the squares of the errors are minimized. A necessary and sufficient condition for equation 34 is,[16]

$$\frac{\partial \bar{S}}{\partial a_j} = 0 \qquad (35)$$

where: a_j = the correlation constants which define the describing mathematical expression.

Equations 35 describe one equation for each correlation constant that is to be determined, thereby uniquely defining the solution.

If the describing mathematical expression is linear in the correlation constants, equations 35 define a system of simultaneous linear equations. The solution to such a system is always obtainable. On the other hand, if the mathematical expression is nonlinear in the correlation constants, equations 35 must be solved by numerical iterative techniques. If the number of equations are large and the form of the equation is complicated, the numerical iterative techniques will not always converge to the solution.[17] It is for this reason that equation 9 is preferred to equation 6 in describing the Froude number effect on centerline temperature excess, as described in Section 1.4.1.1.2.

1.4.1.1.4.2 Centerline Temperature Excess

As shown in Section 1.4.1.1.2, equation 24, which is repeated below, represents the expected form of the relationship among the dimensionless centerline distance, χ, the dimensionless centerline excess temperature, T, the dimensionless lake depth, D, and the densimetric Froude number, F.

$$\chi = \exp\left[\phi + \psi(T-1) + \theta(T-1)^2\right] D^{n_1+n_2(T-1)+n_3(T-1)^2} \exp\left[\beta' \ln F + \gamma' (\ln F)^2\right] \qquad (24)$$

As described in the discussion of statistical methods, it is advantageous to express equation 24 in such a way that the resulting equation is linear in the correlation constants ϕ, ψ, θ, n_1, n_2, n_3, β', and γ'. Such a transformation may be accomplished by taking the natural logarithm of both sides of equation 24. The result is,

$$\ln \chi = \phi + \psi(T-1) + \theta(T-1)^2 + n_1 \ln D + n_2 (T-1) \ln D + n_3 (T-1)^2 \ln D + \beta' \ln F + \gamma' (\ln F)^2 \quad (3$$

The final determination of the equation describing the Ginna data proceeded in steps. The first step involved determining how well the basic χ, T relationship fit the data. The goodness of fit of the mathematical formula to the data was determined by,[18]

$$R = \sqrt{\frac{\sum_{i=1}^{m}\left(y_i-\bar{y}\right)^2 - \sum_{i=1}^{m}\left(y_i-\hat{y}_i\right)^2}{\sum_{i=1}^{m}\left(y_i-\bar{y}\right)^2}} \qquad (37)$$

where:

m = number of data points

y_i = the data point $\ln \chi_i$

$\bar{y}$ = average value of $\ln \chi$ for the m data points

$\hat{y}_i$ = predicted value of $\ln \chi_i$

and R = correlation coefficient.

As can be seen from examining equation 37, R represents the success of the mathematical formulation to predict the data as measured against how well the average of the data describes individual data points. If the mathematical formula is an exact description of the data, R=1. If the formula is no better than using the average of the data, R=0. Therefore, the better the description of the mathematical formula to the data, the greater will be the value of R.

After the correlation coefficient was determined for the basic χ, T relationship,

$$\ln \chi = \phi + \psi (T-1) \qquad (38)$$

additional terms in equation 38 were investigated. For example,

$$\ln \chi = \phi + \psi (T-1) + \theta (T-1)^2 \qquad (39)$$

was next investigated. It was found that this additional term resulted in an insignificant improvement in the data fit. The functional dependence of F on the centerline excess temperature was next investigated by first considering,

$$\ln \chi = \phi + \psi (T-1) + \beta' \ln F + \gamma' (\ln F)^2 \qquad (40)$$

and then considering,

$$\ln \chi = \phi + \psi(T-1) + \beta' \ln F. \qquad (41)$$

It was found that the addition of the Froude number dependence to equation 38 resulted in an insignificant statistical advantage for the surface isotherms. However, equation 41 was seen to provide an improvement in the correlation coefficient for the 6 foot depth isotherms, although equation 40 was no improvement over equation 41.

The effect of dimensionless lake depth, D, on the excess centerline temperature was investigated in a manner similar to the investigation of the densimetric Froude number. It was found that the effect of D on the Ginna isotherms was small. After determining in this way that equations 38 and 41 represented the centerline temperature excess at the surface and 6 feet, respectively, the complete form of equation 36 was checked to see if any synergistic effects existed. The correlation coefficient was found to be substantially unchanged. The final equations, therefore, that were used to describe the centerline temperature excess at Ginna were

$$\ln \chi = \phi + \psi(T-1), \text{ at the surface} \qquad (38)$$

and

$$\ln \chi = \phi + \psi(T-1) + \beta' \ln F, \text{ at 6 foot depth} \qquad (41)$$

The constants ϕ and ψ are, of course, different for the two depths. The values of R for the surface and 6 feet are, 0.784 and 0.746, respectively. The standard deviations, σ, of the independent variable, $\ln \chi$, at the two depths are, 0.351 and 0.374, respectively. Table 1.4-5 summarizes the correlation constants and associated statistical data for the surface and 6 feet.

The form of equation 38 shows that the excess centerline temperature at the surface of the Ginna thermal plume is unaffected by the Froude number and dimensionless lake depth over the range of the Ginna data. This type of behavior was observed by Jen, et al,[19] and Engelund and Pederson,[13] both of whom found that the excess centerline temperature at the surface was dependent only upon the distance from the discharge for large Froude numbers. Shirazi,[6] on the other hand, reports a Froude number dependence, although it is not known whether he investigated the statistical significance of this dependence.

The six foot depth excess centerline temperatures were found to to be affected by the Froude number, although not affected by the dimensionless lake depth except as that variable affects the Froude number. As the Froude number increases, the subsurface centerline

temperature excess increases. This is expected because an increase in Froude number indicates that the inertial forces increase relative to the buoyant forces. This implies that the plume bottom does not rise until later in its development. The higher the Froude number, the longer the plume remains in contact with the six foot depth ambient water. As the Froude number decreases, the longitudinal distance at which the thermal plume separates from the six foot contour decreases. This heat rises to the surface, causing plume spreading to increase, as will be shown in Section 1.4.1.1.4.3.

The statistical results given in Table 1.4-5 show that the mathematical model is a better representation of the surface data than of the six foot data. This reflects the fact that the six foot data actually represents lake depths between 4'11" and 7'1", whereas the surface data were always at a depth of 0'6".

Figure 1.4-10 shows χ vs T for the lake surface. Figure 1.4-11 gives the same information for six foot depth.

1.4.1.1.4.3 Plume Half-Width

The expected form of the plume half width relationship is,

$$r_{0.5}=\exp\left[\alpha+\beta\ln\chi+\gamma(\ln\chi)^2+\delta\ln F+\epsilon(\ln F)^2+\xi\ln D\right] \quad (30)$$

as shown in Section 1.4.1.1.2.3. As described in Section 1.4.1.1.4.1, a form of this equation which is linear in the correlation constants, α, β, γ, δ, ϵ, and ξ, is preferred. Such a form can be obtained by taking the natural logarithm of each side of equation 30. The resulting equation is,

$$\ln r_{0.5}=\alpha+\beta\ln\chi+\gamma(\ln\chi)^2+\delta\ln F+\epsilon(\ln F)^2+\xi\ln D. \quad (31)$$

As in the case of the centerline temperature excess determination, the basic $r_{0.5}$, χ relationship was determined from

$$\ln r_{0.5}=\alpha+\beta\ln\chi. \quad (42)$$

The effect of adding the term in $(\ln\chi)^2$ was then studied. It was found that this effect was significant. The addition of the terms describing F were investigated by studying first,

$$\ln r_{0.5}=\alpha+\beta\ln\chi+\gamma(\ln\chi)^2+\delta\ln F \quad (43)$$

and then, $$\ln r_{0.5}=\alpha+\beta\ln\chi+\gamma(\ln\chi)^2+\delta\ln F+\epsilon(\ln F)^2. \quad (44)$$

It was found, for both the surface and subsurface data, that equation 43 resulted in a definite improvement in the fit to the data, but no further improvement was gained through the addition of the term in $(\ln F)^2$, equation 44. The term in ln D was then considered and found to be statistically unjustifiable. The complete equation 31 was then tried and the correlation coefficient was found to be essentially the same as for equation 43. Therefore, the final form of the plume half width equation was taken as,

$$\ln r_{0.5} = \alpha + \beta \ln x + \gamma (\ln x)^2 + \delta \ln F, \qquad (43)$$

for both surface and six foot depth isotherms.

The correlation constants α, β, γ, and δ are different at the two depths and are given in Table 1.4-5. The correlation coefficients, R, for the surface and six foot depth equations are, 0.647 and 0.600. The standard deviations, σ, of the independent variable, $\ln r_{0.5}$, at the two depths are, 0.481 and 0.570 respectively.

The form of equation 43 indicates that the dimensionless lake depth does not affect the plume half width, except through its effect on the densimetric Froude number. This characteristic was hypothesized in Section 1.4.1.1.2.3 and confirmed by the statistical study. The Froude number behavior, in which δ is less than zero, agrees with that of Shirazi,[6] Jen, et al[19] and Engelund and Pederson.[13] In fact, Jen found the dependence of the half width on the densimetric Froude number at the water surface to be as $F^{-0.25}$. The Ginna data shows this dependence as $F^{-0.264}$.

The fact that the surface plume widths increase with decreasing Froude number was discussed in Section 1.4.1.1.4.2. As the Froude number decreases, the effect of buoyancy increases. Therefore, the plume rises from the six foot contour more quickly, resulting in greater spreading on the surface. This is exactly the behavior predicted by the centerline temperature excess and plume half width relations.

Figure 1.4-12 and 1.4-13 show the plume half widths as a function of centerline distance and densimetric Froude number. The surface isotherms are seen to have half widths always greater than those at six foot depth, illustrating the effect of buoyancy on plume behavior.

1.4.1.1.4.4 Lateral Distribution

As shown in Section 1.4.1.1.2.4, the lateral distribution is expected to have the form,

$$T_m = n \exp\left[-p(r/r_h)^2\right] . \qquad (31)$$

The Ginna lateral distribution can be determined by measuring the r values corresponding to the various isotherms at each centerline point where r_h has been determined. Such an undertaking, however, would be impossible to complete within any reasonable time constraint due to the large number of r values which could be measured (from 3-15 points must be measured for each r_h). Instead of considering all 43 surveys, five surveys were chosen for the lateral distribution analysis. The survey dates were 5/1/70, 12/1/71, 5/14/73, 11/13/73,and 8/4/75. They were chosen so as to represent the range of lake elevations and Froude numbers experienced by the Cinna discharge.

For each centerline point at which the plume half width was measured, values of n and p were determined for $0.5 \leq T_m \leq 1$ and $T_m \leq 0.5$ in accordance with equations 31 and 33, the latter being,

$$n = 0.5 \exp(p) \qquad (33)$$

Equation 33 results from the fact that $r = r_h$ at $T_m = \Delta T/\Delta T_c = 0.5$, as shown in Section 1.4.1.1.2.4.

The values of n and p were determined from a least squares fit of the studied lateral distributions, of which there were 23 in the five surveys. It was found that p=0.661 described the distributions for $0.5 < T_m < 1$ and p=0.663 described the distributions for $T_m < 0.5$. As described in the analytical discussion, the fact that $T_m = 1$ when $r = 0$ and $T_m = 0.5$ when $r = r_h$ implies that $p = \ln 2 = 0.693$. Table 1.4-6 compares the lateral distributions found from the Ginna data with that of a normalized Gaussian (n=1, p=ln 2). It is seen that, except for values of T_m near one, the normalized Gaussian is virtually the same as the Ginna distribution. Since it was shown that the normalized Gaussian must apply for the region $0.5 \leq T_m \leq 1$, and since the two distributions are almost identical except for the small region where $T_m \approx 1$, the normalized Gaussian is taken as the appropriate distribution. That is

$$T_m = \exp\left[-\ln 2(r/r_h)^2\right] \qquad (45)$$

describes the lateral temperature distribution. This distribution is the one most frequently used by investigators of thermal plumes. (3,6,8,11,14) Figure 1.4-14 is a graphical depiction of the lateral distribution, equation 45.

1.4.1.1.4.3 Possible Sources of Data Scatter

Scatter in the correlation model may result from either inadequacies in the model or inaccuracies in the data. Inadequacies in the model would stem from neglecting important mechanisms which affect the thermal distribution. The major model assumption was that Lake Ontario currents do not affect the thermal plume except for a gradual bending of its trajectory. Such an assumption was shown to be valid for current velocities much less than the discharge velocity, a condition normally expected at Ginna. Greater current velocities result in increased mixing with the ambient in addition to the bending of the jet trajectory. Any increase in ambient entrainment was not accounted for by the correlation model. Section 1.4.1.1.2 discusses the other mechanisms which affect the Ginna thermal plume.

Data inaccuracies are inherent in any sampling program. The inaccuracies of the temperature measuring devices, inaccuracies in boat position and speed determinations, and inaccuracies in the determination of sampling depth due to the presence of waves cannot be eliminated.

A perhaps more important data error source lies in the determination of ambient temperatures and therefore the determination of excess temperatures. The ambient temperature for each survey was obtained by sampling offshore of the thermal plume. However, Chermack and Galletta (20) found that the undisturbed ambient at Ginna always exhibits a horizontal thermal gradient between the shoreline and 5000 feet offshore. When this gradient is positive, as it is from March until August, the Ginna data excess temperatures are overstatements of their actual value. When the gradient is negative, as it is from September until February, the Ginna data excess temperatures are understatements of their true value. Table 1.4-7 shows the monthly temperature difference found by Chermack and Galletta between the shoreline and 5000 feet offshore in the vicinity of the Ginna site for the years 1969-1972. It is seen that the yearly average gradient is $+0.6^{\circ}F$ between these points. Of the Ginna thermal surveys, 60% were sampled during positive gradient months and 40% during negative gradient months. The average gradient between the shoreline and 5000 feet offshore for all of the thermal surveys was $+0.7^{\circ}F$, thereby indicating that the overall effect of the horizontal

temperature gradient is to make the excess temperature data conservatively high, although the opposite will be true for thermal surveys taken between September and February. In practice, no surveys are taken in January and February.

1.4.1.1.5 Model Application

1.4.1.1.5.1 Isotherm Construction

The first step in constructing isotherm maps from the mathematical model is a specification of the ambient conditions. Lake elevation and ambient temperature uniquely determine, for a constant temperature rise, the densimetric Froude number, F, and linear scale factor, $\sqrt{a/2}$, for a given discharge. The values at Ginna of the latter two parameters may be found from Figures 1.4-15 and 1.4-16 or calculated directly from their definitions. Note that the densimetric Froude numbers given in Figure 1.4-15 assume the Ginna design discharge excess temperature of 20°F. Dimensionless temperature excesses, T, along the plume trajectory, λ, are then found from either Figure 1.4-10 or equation 38 for surface isotherms and either Figure 1.4-11 or equation 41 for six foot depth isotherms. At each location along the plume centerline, dimensionless half widths, $r_{0.5}$, are calculated from equation 43 or Figures 1.4-12 (surface) and 1.4-13 (six foot depth). Multiplication of the dimensionless half widths and centerline distances by the linear scale factor and of the dimensionless centerline temperature excess by the discharge temperature excess, ΔT_o, results in the corresponding dimensioned variables, r_h, s, and ΔT_c. Use of Figure 1.4-14 or equation 45 then allows the calculation of the temperature excess at various distances normal to the centerline for each value of s and the corresponding value of r_h and ΔT_c. Within the core region, T=1, the lateral temperature profile changes from a constant to Gaussian. No data are available within this region. It can be assumed that the isotherms spread linearly between the discharge and the end of the core region.

1.4.1.1.5.2 Worst Case Isotherms

The surface and subsurface isotherms described in Section 1.4.1.1.5.1 are derived from expected values of the dimensionless centerline temperature excess and half width. However, due to data scatter, any single measurement will normally not conform to its expected value. This data behavior can be described by considering confidence limits around the expected value. That is, any single measurement may not conform to its expected value but it will have a certain probability, the confidence limit, of being within a specified range. The probability chosen for the confidence limit is frequently 0.95, or 95%. This confidence limit allows one to state with reasonable certainty that a single

measurement will lie within a physically meaningful data range.

If two variables were directly proportional, the probability that both would exceed their 95% upper confidence limit would be the same as the probability that one would exceed its 95% upper confidence limit. If two variables were totally independent, then the probability that either will exceed its 77.6% upper confidence limit is 0.224, but the probability that both will exceed their 77.6% upper confidence limit is 0.95. Expressed another way, if two variables are directly proportional, their combined 95% upper confidence limit is the 95% upper confidence limit of each; whereas, if two variables are independent, their combined 95% upper confidence limit is the 77.6% upper confidence limit of each. Next, consider the case of two inversely proportional variables. The probability that both will exceed their 95% upper confidence limit is virtually zero since as one increases from its expected value toward its 95% upper confidence limit the other will decrease.

In this analysis we are dealing with a case which is intermediate of the latter two cases described in the previous paragraph. As found by all investigators of the thermal plume phenomenon, for a given set of discharge conditions, half widths will always decrease with increasing isotherm lengths. Indeed, this must be true because a constant heat rejection rate implies a constant plume heat flux. Due to the many factors which affect thermal plumes, it is not possible to quantify this inverse relationship. The joint 95% upper confidence limit of centerline temperature excess and half width, therefore, cannot be quantified. However, an upper confidence limit can be ascribed to these variables. If the centerline temperature excess or plume half width were at its 95% upper confidence limit, the other variable should be less than its expected value due to the inverse relationship described above. A 95+% upper confidence limit (the exact confidence value is not determinable) can therefore be taken as either variable at the upper range of its 95% confidence limit with the other variable at its expected value. The resulting isotherms can be labelled "worst case."

Isotherm areas were calculated for the 95% confidence limit of centerline temperature excess with the expected plume half width and vice versa. Results from the former case indicated 3°F surface isotherm areas approximately 10% larger than the latter. Therefore, the former case is used to quantify "worst case" isotherm effects.

1.4.1.2 Comparison of Model With Data

As explained in Section 1.4.1.1.5.2, an individual measurement may not be equal to its expected value. The measurement must, therefore, be compared with some confidence range, 95% being chosen. Figures 1.4-6 through 1.4-9 show typical surface and six foot centerline temperature excess and plume half width data. Also shown are the 95% confidence limits corresponding to the ambient conditions prevalent on each date. Note that all of the data lies within the chosen confidence limits. Figure 1.4-8, surface data on 5/1/70, was specifically chosen in order to illustrate a case where centerline temperature excess data may be near their upper confidence limit. Note, however that the half width data are near their expected values. Most of the other data points are near their expected values, except for a few surface half width points on 10/27/71. Here again the centerline temperature excess data are near their expected values.

Section 1.4.2.6 gives the plume size for a wide range of ambient conditions. As will be shown there, the worst case plume will have a 3°F surface area ranging up to approximately 470 acres. This can be compared with the largest 3°F area ever noted during the Ginna thermal surveys of 235.2 acres. The worst case plume will have a area at six foot depth ranging up to approximately 160 acres. This can be compared with the maximum value actually observed at Ginna of 120.4 acres. This illustrates the fact that the worst case plume is actually a 95+% confidence limit, as explained in Section 1.4.1.1.5.2. The above figures are exclusive of winter, when ambient conditions are such that the plume will sink. As explained in Section 1.4.1.1.3.2, the model has not been derived for these conditions. However, winter plume effects are addressed in Section 1.4.2.

As described in Section 1.4.1.1.3, Ginna thermal survey data taken from 5/1/70 through 8/4/75 were used to develop the mathematical model. Eight surveys were performed during the period from 9/11/75 through 11/5/76. These surveys were used as an independent check of the model. Three of the eight surveys had no 3°F isotherm existing at the six foot level. Three others had six foot thermal distributions which did not emanate from the discharge, an underlying assumption of the model. It is of interest to note, however, that these latter three had 3°F six foot depth areas 31, 33 and 92% of that given by worst case plume predictions corresponding to their ambient and discharge conditions.

The remaining two six foot depth temperature distributions along with the eight surface distributions were reduced to dimensionless form in the manner described in Section 1.4.1.1.3. Figures 1.4-17 through 26 show this data along with their associated 95% confidence limits. Two half width data points at the six foot depth and one point at the surface lie slightly outside the 95% confidence range on 10/21/75. Note that the corresponding

centerline temperature excesses are near their expected value. These large half widths can be attributed to uncertainty in determining the plume trajectory. A different plume trajectory would result in different values of the dimensionless variables.

A number of centerline temperature excess data points at high excess temperatures are less than the low end of the 95% confidence range. These, together with the three surveys which showed no 3°F excess temperatures at six foot depth, is evidence suggesting that the model may be somewhat of an overstatement of the thermal plume size at Ginna. If the surveys performed subsequent to 8/4/75 were integrated into the model, predicted isothermal areas would probably be somewhat smaller than those given in this study.

1.4.2 THERMAL EFFECTS OF DISCHARGE

1.4.2.1 Ambient Conditions

As explained in Section 1.4.1, the temperature distribution resulting from the Ginna discharge will depend upon the lake elevation and lake temperature. Lake elevations were obtained from the daily records of NOAA's Rochester gaging station for the period from January 1953 through December 1976.[15] Lake temperatures were determined from the daily records of the Ginna intake water temperature for the period from January 1970 through November 1976.

Seasonal elevations and temperatures were determined from the daily records. The winter, spring, summer, and fall seasons were taken as consecutive three month periods beginning with January. Table 1.4-8 gives the seasonal lake temperatures and elevations.

1.4.2.2 Lake Bottom Temperature Rise

In May 1974, RG&E sponsored 3 field surveys to determine discharge induced lake bottom temperatures and velocities at the Ginna site. (See Section 1.4.3.1.2 for a discussion of bottom velocities). Excess temperatures and associated areas from these surveys were nondimensionalized in a manner similar to that described in Section 1.4.1.1. The relationship between excess temperatures and areas, for the conditions existing while the measurements were being performed, was found to be,

$$A_a = -18.86 \frac{\Delta T}{\Delta T_o} + 9.49 \qquad (46)$$

and

$$A_m = -20.72 \frac{\Delta T}{\Delta T_o} + 13.35, \qquad (47)$$

where A_a = area of isotherm whose excess temperature is ΔT, average of field measurements (acres)
A_m = area of isotherm whose excess temperature is ΔT, maximum of field measurements (acres)
ΔT = excess temperature
and ΔT_o = discharge excess temperature.

Equations 46 and 47 were determined for values of $\Delta T/\Delta T_o$ between approximately 0.17 and 0.37. This corresponds to temperature excesses from approximately 3 to 7°F for a discharge excess temperature of 20°F.

The conditions existing during the field measurements were equivalent, for a discharge excess temperature of 20°F, to a lake elevation of 248.7 feet USGS and a lake temperature of 40°F. It can be assumed that the area-temperature behavior along the lake bottom follows the subsurface, six foot depth plume behavior determined in Section 1.4.1.1.4. In this manner, equations 46 and 47 will be extended to ambient conditions other than those existing during the measurements.

Although not enough information is available to define lake bottom isotherm shapes, two items of interest were noted. Firstly, the extent of the isotherms will range from approximately 700 feet for the 7°F isotherm to approximately 1000 feet for the 3°F isotherm. Secondly, the maximum widths of the isotherms occur at approximately 0.75 of the total distance along the centerline.

1.4.2.3 Velocity Decay

The decay of velocity along the path of the plume can be estimated from the temperature decay. In the near field, plume temperatures are decreased chiefly by mixing with the cooler ambient water. Some heat is also lost to the atmosphere, but, as shown in Section 1.4.1.1.2.1, this contribution is small. The decrease in plume velocity arises, as does the decrease in temperature, chiefly from mixing with the lower momentum ambient water. Therefore, it can be postulated that, in the near field, the dimensionless velocity decays in the same way as the dimensionless temperature.[14] This can be expressed as,

$$\frac{U}{U_o} = \frac{\Delta T}{\Delta T_o} \qquad (48)$$

where U = plume excess velocity
and U_o = discharge velocity.

Given the temperature decay and the discharge velocity, it is therefore possible to calculate the velocity at any point in the plume. Figure 1.4-27 shows the discharge velocity, which depends only on the lake elevation, for the range of conditions encountered at the site.

1.4.2.3.1 Exposure Time

The use of equation 48 in conjunction with the temperature decay determined in Section 1.4.1.1.4 allows determination of the time it takes for a parcel of water to cool to a given temperature. If this calculation is performed along the plume's surface centerline during still water conditions, maximum exposure times

result. The relationship between time, distance, and velocity is,

$$\int_{t_o}^{t} dt = \int_{o}^{s} \frac{1}{U}\, ds, \qquad (49)$$

where t_o = travel time from condenser entry to lake discharge
t = travel time from condenser entry to s
s = distance along path of plume measured from lake discharge.

If equation 48 is substituted into 49, the result is,

$$t = t_o + \frac{\Delta T_o}{U_o} \int_{o}^{s} \frac{1}{\Delta T}\, ds \qquad (50)$$

where ΔT is a function of s. Note that ΔT at the centerline is given in Table 1.4-5.

1.4.2.3.2 Plume Trajectory

It is explained in Section 1.4.1.1.2.1 that the effect of the ambient currents, for the normally occurring current range at Ginna, is a gradual bending of the plume's trajectory. Since the model described in Section 1.4.1.1 is derived in terms of centerline distances along the path of the plume, the temperature distribution in the presence of an ambient current can be estimated from knowledge of the plume's trajectory.

The absolute velocity along the centerline of plume is the resultant of the plume and ambient velocity components. For an ambient velocity perpendicular to the discharge velocity, this leads to the expressions,

$$\sin \theta = \frac{U_c}{\sqrt{U_c^2+U_a^2}} \qquad (51)$$

and

$$\cos \theta = \frac{U_a}{\sqrt{U_c^2+U_a^2}} \qquad (52)$$

where U_c = plume centerline excess velocity
U_a = ambient velocity
θ = angle between the ambient velocity component and the resultant velocity
and $\sqrt{U_c^2+U_a^2}$ = resultant velocity.

If x is taken as the direction of the discharge and y as the direction of the ambient current, then

$$\frac{dx}{ds} = \sin\theta \tag{53}$$

and

$$\frac{dy}{ds} = \cos\theta \tag{54}$$

Substituting equations 51 and 52 into 53 and 54, respectively, and integrating both sides yields,

$$x = \int_0^s \frac{U_c}{\sqrt{U_c^2+U_a^2}}\, ds \tag{55}$$

and

$$y = \int_0^s \frac{U_a}{\sqrt{U_c^2+U_a^2}}\, ds\ , \tag{56}$$

where x, y , and s are measured from the center of the discharge plane. Note that U_c can be calculated as a function of s by use of equation 48 and the information in Table 1.4-5.

1.4.2.4 Winter Recirculation

When intake temperatures drop below 40°F, such as occurs during the winter, discharge water is recirculated so that the condenser inlet water temperature is 40°F. This has the effect of lowering the flow rate of the discharge to the lake while raising the discharge excess temperature. Figure 1.4-28 shows the discharge flow rate and excess temperature as a function of ambient (intake) temperature.

Although the model developed in Section 1.4.1.1 is not directly applicable to ambient temperatures much below 40°F, it can be used as an indicator of the size of the winter plume. This is because

the basic mechanisms which govern plume dilution are similar whether the plume is buoyant or not. That is, dilution is governed by the mixing properties of the plume with the ambient. The major differences between the buoyant and non-buoyant cases are the buoyant plume will lose heat to the atmosphere while the non-buoyant plume will exhibit more complete vertical mixing. As shown in Section 1.4.1.1.2.1, the former difference is unimportant. The latter difference will cause a deepening of the thermal field. However, the increased vertical mixing will also result in more rapid decay of the discharge temperatures.

In the sections which follow, plume areas along the surface and six foot depth are presented for the winter season. The calculations are based on the model of Section 1.4.1.1 and are intended only as general guides to the overall extent of the thermal field. They are, accordingly, indicated as dashed lines in the appropriate figures. Volumes have also been calculated. These are shown as solid lines in order to demonstrate that, although the vertical trajectory of the winter plume makes the surface and six foot depth areas only general indications of plume extent, the volumes, or overall plume size, will be better approximations.

1.4.2.5 Seasonal Thermal Effects

Thermal effects of the Ginna discharge during normal (expected) and extreme (worst case) seasonal conditions follow. Figures describing the seasonal thermal effects are arranged by type rather than season. Figures 1.4-29 through 40 illustrate surface and six foot depth isotherm maps for the seasonal cases. Figures 1.4-41 through 44 give the corresponding isotherm areas, while Figure 1.4-45 relates lake bottom isotherm areas. Figure 1.4-46 shows isotherm volumes, 1.4-47 through 52 gives exposure times, and 1.4-53 through 58 illustrates plume trajectories.

All plume calculations assume a vertically uniform ambient temperature. If the ambient temperatures are not vertically uniform, such as occurs in the summer, the plant will take in colder water than will be seen by the discharge. This means that the discharge excess temperature will be decreased by the amount of stratification between the intake and discharge levels. This will reduce the thermal effects of the discharge for two reasons. First, the lower discharge excess temperature means lower excess temperatures throughout the plume's development. Second, the lower discharge excess temperature lowers the buoyancy of the plume, thus resulting in greater discharge diluting capabilities. Neglect of ambient stratification, therefore, results in conservatively large summer plume predictions.

1.4.2.5.1 Expected Seasonal Conditions

Expected seasonal conditions, given in Table 1.4-8, are defined as the expected plume under average ambient conditions.

1.4.2.5.1.1 Expected Winter Plume

As explained in Section 1.4.2.4, the mathematical model was not derived for winter conditions. Because of the uncertainty in plume configuration, no isotherm maps were drawn. Figures 1.4-41 and 42 show surface and six foot depth areas calculated from the model. These areas are presented to give a general idea as to plume extent and are indicated as dashed lines, as described in Section 1.4.2.4. Figure 1.4-46 gives the expected winter volumes, as calculated from the model. As noted in Section 1.4.2.4,these values are larger than those which will occur, due to the increased vertical mixing caused by the decreased buoyancy effects.

1.4.2.5.1.2 Expected Spring Plume

Figures 1.4-29 and 30 show the expected surface and six foot depth isotherms. Figures 1.4-41 and 42 give the corresponding areas. Figure 1.4-45 gives the area along the lake bottom,

while volumes can be found from Figure 1.4-46. The 3°F isotherm has areas on the surface, six foot depth and bottom of 86, 32, and 5.6 acres, with a volume of 460 acre-feet. Figure 1.4-47 shows that the maximum time a parcel of water will be at 3°F or higher is 42 minutes.

Figure 1.4-53 shows the plume trajectory for alongshore currents of 0.17, 0.33, and 0.50 fps. Note that these trajectories do not take into account the presence of Smoky Point. Alongshore ambient currents will be deflected into the body of the lake due to the existence of Smoky Point. This phenomenon is not accounted for here. The trajectory curves assume an undeflected ambient current direction.

1.4.2.5.1.3 Expected Summer Plume

Figures 1.4-31 and 32 show the surface and six foot depth isotherms. 3°F areas along the surface, six foot depth, and bottom, as found in Figures 1.4-41, 42, and 45, are 87, 27, and 4.6 acres, respectively. The 3°F volume, as found in Figure 1.4-46, is 420 acre-feet. The 3°F exposure time, found in Figure 1.4-48, is 39 minutes. Figure 1.4-54 shows the plume trajectories for currents up to 0.5 fps. As noted in Section 1.4.2.5, these thermal effects are conservatively large in that ambient vertical temperature stratification is not considered.

1.4.2.5.1.4 Expected Fall Plume

Table 1.4-8 shows the expected fall lake elevation to be over one foot lower than the spring and summer elevations. The resulting larger discharge velocity, in conjunction with the low ambient temperature, can be expected to cause a decrease in the plume size. This decrease should be most pronounced at the surface, as the increase in Froude number will increase plume mixing. Subsurface areas, however, will also be affected by the decrease in buoyant plume rise.

Expected fall isotherms can be found on Figures 1.4-33 and 34. 3°F areas, found on the same figures as the other expected seasonal conditions, are 63, 30, and 5.1 acres, corresponding to the surface, six foot depth, and bottom, respectively. The 3°F volume is 380 acre-feet. Note that, as expected, the overall plume size has decreased from the spring and summer, although the subsurface areas have not.

The maximum 3°F exposure time is 30 minutes, as seen in Figure 1.4-49. Figure 1.4-55 shows the plume trajectories.

1.4.2.5.2 Extreme Seasonal Conditions

Extreme seasonal conditions were defined as high lake elevations and high lake temperatures, both conditions being conducive to low rates of plume thermal decay. For the winter, when discharge-intake recirculation occurs, the lowest ambient temperature results in the largest thermal field due to the increase in excess temperature and decrease in discharge velocity. Seasonal extreme elevations and temperatures were taken as the daily extreme found in the entire record described in Section 1.4.2.1. These ambient conditions were combined with the "worst case" plume predictions described in Section 1.4.1.1.5.2 and the maximum bottom areas described in Section 1.4.2.2. The result can be considered an upper limit to the size of the Ginna plume. It should be noted that most plumes will exhibit behavior similar to the expected plumes, with the frequency of occurrence sharply decreasing as extreme plume behavior is approached. Table 1.4-8 shows the extreme seasonal conditions.

1.4.2.5.2.1 Extreme Winter Plume

As explained in Section 1.4.2.4, the mathematical model was derived for buoyant plume behavior. During the winter, the negative buoyancy of the plume makes its configuration uncertain. Figures 1.4-43, 44 and 46 show the surface and six foot depth isothermal areas along with the volumes. As noted in Section 1.4.2.4, these values are conservatively large.

1.4.2.5.2.2 Extreme Spring Plume

Figures 1.4-35 and 36 show the surface and six foot depth isotherm maps. Figures 1.4-43 and 44 give the corresponding areas for each season. Figures 1.4-45 and 46 give the seasonal lake bottom areas and volumes, respectively, for all seasonal conditions. The surface, six foot depth, and bottom $3^{\circ}F$ areas are 463, 133 and 9.5 acres, respectively. The $3^{\circ}F$ volume is 2100 acre-feet. The maximum $3^{\circ}F$ exposure time, shown in Figure 1.4-50, is 155 minutes. Plume trajectories are given in Figure 1.4-56.

1.4.2.5.2.3 Extreme Summer Plume

Figures 1.4-37 and 38 show the extreme summer plant induced thermal distributions. $3^{\circ}F$ areas are 396, 119, and 8.5 acres, for the surface, six foot depth, and bottom, respectively. The $3^{\circ}F$ volume is 1800 acres. Figure 1.4-51 gives the $3^{\circ}F$ exposure time as 126 minutes. Figure 1.4-57 gives plume trajectories. As noted in Section 1.4.2.5, these thermal effects do not account for vertical temperature stratification in the ambient. Consideration of this phenomenon would lower the predicted effects of the summer plume.

1.4.2.5.2.4 Extreme Fall Plume

As in the case of the expected conditions, extreme fall conditions have lake elevations much less, more than two feet less in this case, than the extreme spring and summer conditions. In addition, the extreme fall lake temperature is much less than that of the extreme spring and summer. The result will be a decrease in plume size, chiefly reflected in near surface areas. 3°F surface, six foot depth, and bottom areas are 257, 111, and 7.9 acres, respectively. The 3°F volume is 1400 acres. The 3°F exposure time, as found from Figure 1.4-52 is 84 minutes, reflecting the relatively large discharge velocity and the rapid temperature decay. Extreme fall plume trajectories are given in Figure 1.4-58.

1.4.2.6 Parametric Thermal Plume Analysis

As shown in Section 1.4.1.1, of the factors which might affect the Ginna plume, only variations in lake elevations and temperatures will cause major variations in the size of the discharge plume. As the lake elevation increases, the discharge velocity decreases. This results in a decrease of the mixing capabilities of the plume. As the lake temperature increases, the nonlinear temperature-density relationship of water causes an increase in plume buoyancy. This behavior inhibits plume mixing and causes the plume to spread on the lake surface.

Surface and six foot depth isothermal areas were calculated for lake elevations of 244 to 250 feet USGS and lake temperatures of 40 through 80°F. Results for lake temperatures below 40°F, which include discharge-intake recirculation effects, are also shown for completeness. As indicated in Section 1.4.2.4, areas for ambient temperatures less than 40°F should be interpreted as indications of overall plume size. These areas are also useful in determining isothermal volumes, which will give a better, but still conservatively large, idea of the overall plume size for lake temperatures less than 40°F. It is of interst to note that surface isotherm areas decrease with decreasing lake temperature. However, below 40°F, surface isotherm areas will increase with decreasing lake temperatures due to winter recirculation (see Section 1.4.2.4). This behavior is noted on the figures discussed below.

Figures 1.4-59 through 62 show expected 2,3,5 and 10°F surface areas. For the range of conditions considered, other than winter, these values range from 56 to 225 acres, 41 to 167 acres, 24 to 97 acres, and 6.7 to 27 acres, respectively. As explained above, the isothermal areas increase with increasing lake temperatures and elevations. Figures 1.4-63 through 66 show expected 2,3,5 and 10°F six foot depth areas. For the non-winter conditions, these areas range from 31 to 57 acres, 22 to 40 acres, 12 to 20 acres, and 2.7 to 4.0 acres, respectively. Six foot depth areas increase with increasing lake elevation but decrease with increasing lake temperature. The former shows the effect of the

decreased mixing caused by the decrease in discharge velocity. The latter is caused by an increase in plume buoyancy, causing the plume to rise from the six foot level earlier in its development. This increase in buoyant rise causes an increase in surface areas but a decrease in subsurface areas.

Figures 1.4-67 through 69 show isothermal areas along the lake bottom for lake temperatures between 40 and 80°F and lake elevations between 244 and 250 feet USGS. 3°F expected bottom areas range from 3.8 to 6.9 acres. The behavior of the lake bottom isotherms with varying temperatures and elevations is the same as the behavior of the six foot depth isotherms.

Figures 1.4-70 through 73 show worst case 2,3,5, and 10°F excess temperature areas along the surface. For the same range of lake elevations and lake temperatures considered for the expected plume discussion, these areas range, in acres, from 150 to 606, 116 to 471, 74 to 298, and 25 to 100, respectively. Six foot depth areas, shown in Figures 1.4-74 through 77, range from 100 to 216 acres, 75 to 159 acres, 45 to 90 acres, and 13 to 23 acres, respectively. Maximum 3°F lake bottom areas range from 5.4 to 11.3 acres.

Parametric isothermal volumes can be estimated from the surface and six foot depth isothermal area information. Note that lake bottom areas are always much less than six foot depth areas. Using the trapezoidal integration rule and assuming zero areas at 10 foot depth yields,

$$V = 3A_0 + 5A_6 \qquad (57)$$

where V = volume (acre-feet)

A_0 = surface area (acres)

and A_6 = six foot depth area (acres).

The use of equation 57 gives approximate 3°F expected volumes from 260 to 630 acre-feet for lake temperatures from 40 to 80°F and elevations from 244 to 250 feet USGS. 3°F worst case volumes range from 760 to 2000 acre-feet.

The centerline time-temperature decay of expected and worst case plumes were calculated for lake elevations of 244 through 250 feet USGS. As shown in Table 1.4-5, the surface centerline temperature decay is independent of Froude number, and, therefore, ambient temperature. Since it was assumed that the excess velocity decays in the same way as excess temperature, the

calculated centerline surface exposure times are independent of ambient temperature. As shown in Figures 1.4-78 through 81, 3°F exposure times range from 21 to 76 minutes for the expected plume and 40 to 149 minutes for the worst case plume. The larger elevations result in longer exposure times because the discharge velocities are lower.

1.4.3 PHYSICAL EFFECTS OF DISC...

1.4.3.1 Velocity Effects

1.4.3.1.1 Surface Velocities

As explained in Section 1.4.2.3, plume surface velocities can be assumed to decay in the same manner as plume surface temperatures. Discharge excess temperature has been taken as $20^{\circ}F$ for all conditions except lake temperatures less than $40^{\circ}F$. Discharge velocity, on the other hand, varies with lake elevation, as shown in Figure 1.4-27.

Table 1.4-9 shows the surface excess velocity decay for seasonal conditions, as a function of distance along the plume trajectory. It is of interest to note that higher discharge velocities result in greater mixing of the discharge and ambient cooling water. This results in a greater velocity decay rate. Expected seasonal conditions show excess velocities of the same magnitude as the lake approximately 4000 feet from the discharge. This distance is approximately 8000 to 9000 feet for the extreme conditions.

1.4.3.1.2 Bottom Velocities

In May 1974, RG&E sponsored 3 field surveys to determine discharge induced lake bottom temperatures and velocities at the Ginna site. (See Section 1.4.2.2 for a discussion of bottom temperatures.) Velocities and areas were reduced to dimensionless form and the relationship between them determined. The result was,

$$A_a = -20.84\frac{U}{U_o} + 9.20, \quad .36 > U/U_o > .18 \qquad (58)$$

and

$$A_m = -39.62\frac{U}{U_o} + 17.30, \quad .36 > U/U_o > .18 \qquad (59)$$

where

U = bottom velocity

U_o = discharge velocity

A_a = area of isopleth of velocity U, average of field measurements (acres)

and A_m = area of isopleth of velocity U, maximum of field measurements (acres).

The areas determined from equations 58 and 59 were applied to conditions other than those existing during the field measurements by multiplying by appropriate scale factor ratios. Figure 1.4-82 shows average and maximum lake bottom scour areas, defined as areas along the lake bottom where the velocity is greater than 1 fps, for lake elevations from 244 to 250 feet USGS. Average scour areas range from 0.4 to 2.8 acres; maximum areas range from 0.5 to 5.2 acres. Spring, summer, and fall expected seasonal conditions correspond to average areas of 2.6, 2.6 and 2.8 acres, respectively. The higher area for fall reflects the lower lake elevation. Spring, summer, and fall extreme seasonal conditions correspond to maximum areas of 0.1, 2.4, and 4.7 acres, respectively. The low value for spring results from the high lake elevation, 250.19 feet USGS.

1.4.3.2 Concentrations

It is possible to determine the characteristics of chemical dilution in the Ginna discharge by drawing the analogy between temperature and chemical dilution. Both are chiefly products of mixing of discharge and ambient water. Temperature decay also occurs by atmospheric cooling but, as shown in Section 1.4.1.1.2.1, this is unimportant in the near field.

The characteristics (isopleth shape, area, and volume) of the chemical dilution will be the same as the characteristics of the thermal dilution if the dimensionless excess concentration is equal to the dimensionless excess temperature. That is,

$$\frac{C - C_a}{C_o - C_a} = \frac{\Delta T}{\Delta T_o} \quad , \tag{60}$$

where C = concentration
C_a = ambient concentration
C_o = discharge concentration
ΔT = excess temperature
and ΔT_o = discharge excess temperature.

Equation 60 can be used to relate concentration characteristics with the thermal characteristics developed in Section 1.4.2. If equation 60 is satisfied, then the isopleth of concentration C will have the same shape, area, and volume as the isotherm of excess temperature ΔT.

1.4.3.3 Shoreline Erosion

The major erosion effect of the Ginna discharge is bottom scouring in the vicinity of the discharge. This has been discussed in Section 1.4.3.1.2, where it was shown that scoured areas may range from 0.4 to 5.2 acres, depending on lake and discharge conditions. It should be noted that the scour areas exhibit shapes similar to isotherm shapes, their major influence being directed offshore.

It is also possible to postulate that a shoreline discharge of water, such as exists at Ginna, can act as a barrier to movement of lake sediments. If the discharge were to give the same effects as a solid barrier, deposition would occur upstream of the discharge and erosion would occur downstream of the discharge. However, a number of factors mitigate this behavior.

Currents at the site are alternately in both alongshore directions with a predominance of west to east currents. This would cause alternate erosion and deposition on either side of the discharge, with a small net effect. Furthermore, the plume completely blocks the normal alongshore flow for a distance of approximately 1000 feet offshore. After this point, the alongshore flow can pass under the plume.

No shoreline erosion due to discharge operation has been noticed since Ginna began operating in 1969.